Published for SISSA by Springer

Received: *April 5, 2025*
Accepted: *July 2, 2025*
Published: *August 4, 2025*

Modular transport in two-dimensional conformal field theory

Mihail Mintchev[a], **Diego Pontello**[b] **and Erik Tonni**[b]

[a] *Dipartimento di Fisica, Università di Pisa and INFN Sezione di Pisa, largo Bruno Pontecorvo 3, 56127 Pisa, Italy*
[b] *SISSA and INFN Sezione di Trieste, via Bonomea 265, 34136, Trieste, Italy*

E-mail: mintchev@df.unipi.it, diegopontello@gmail.com, etonni@sissa.it

Abstract: We study the quantum transport generated by the bipartite entanglement in two-dimensional conformal field theory at finite density with the U(1) × U(1) symmetry associated to the conservation of the electric charge and of the helicity. The bipartition given by an interval is considered, either on the line or on the circle. The continuity equations and the corresponding conserved quantities for the modular flows of the currents and of the energy-momentum tensor are derived. We investigate the mean values of the associated currents and their quantum fluctuations in the finite density representation, which describe the properties of the modular quantum transport. The modular analogues of the Johnson-Nyquist law and of the fluctuation-dissipation relation are found, which encode the thermal nature of the modular evolution.

Keywords: Field Theories in Lower Dimensions, Scale and Conformal Symmetries, Non-Equilibrium Field Theory

ArXiv ePrint: 2503.16368

Dedicated to the memory of Ivan Todorov

https://doi.org/10.1007/JHEP08(2025)021

JHEP08(2025)021

Contents

JHEP08(2025)021

1 Introduction

Entanglement is a fundamental property of quantum systems which can be investigated e.g. by considering a spatial bipartition identified by a subsystem A and its complement B. Assuming that the Hilbert space is factorised accordingly and denoting by ρ the state of the entire system, the reduced density matrix $\rho_A \equiv \mathrm{Tr}_B \rho$ obtained by tracing out the degrees of freedom associated to B determines an intrinsic internal dynamics known as modular evolution [1]. This evolution is generated by the modular Hamiltonian K_A of the subsystem, which is defined as $\rho_A \sim \mathrm{e}^{-K_A}$ and depends on the representation of the theory. A basic feature of the evolution of any quantum system is the existence of conserved charges. Their propagation in spacetime is implemented by the corresponding currents, which generate the quantum transport [2–4]. In this paper we study the conserved charges, the currents and transport properties associated to the modular evolution.

The modular Hamiltonian is known analytically in very few cases. The most important one corresponds to the theorem of Bisognano and Wichmann [5, 6], which considers the bipartition associated to half space of a local relativistic quantum field theory in its fundamental representation. Another important class of examples is given by conformal field theories (CFT) in two spacetime dimensions, where some modular Hamiltonians K_A of an interval A are explicitly known and take a local form in various inequivalent representations [7–11].

In two-dimensional CFT, besides the fundamental representation, where the quantum transport is rather trivial, other representations at finite particle density and/or finite temperature have been explored [12–17]. When the left and right moving excitations have different temperature, the underlying states are non-equilibrium steady states (NESS) [18–20] and display interesting transport properties [13–16, 21]. Focussing on the zero temperature case for the sake of simplicity, in this paper we study the modular evolution generated by the modular Hamiltonian of an interval A for a CFT in the state characterised by non-vanishing chemical potentials and investigate the corresponding quantum transport.

We consider a local CFT in $1+1$ spacetime dimensions with $\mathrm{U}(1) \times \mathrm{U}(1)$ symmetry, implementing the electric charge and the helicity conservation. Along the modular flow, conformal invariance fixes the one-point and two-point functions. In this way one determines the mean values of the currents and their quadratic quantum fluctuations (noise), which provide a physical picture the modular quantum transport in the system.

The paper is organised as follows. In section 2 we discuss the evolution of the basic CFT chiral fields generated by a Hamiltonian depending on a smooth inhomogeneous velocity for each chirality. In section 3 these evolutions are employed to construct currents, continuity equations and conserved quantities in this inhomogeneous CFT. In section 4 we consider the modular evolution for a CFT on the line in the finite density representation and the bipartition determined by an interval is considered and in section 5 the corresponding modular transport properties are investigated. In section 6 and section 7 these analyses are performed

JHEP08(2025)021

for the finite density representation of a CFT at finite volume. Some conclusions are drawn in section 8. Further results and technical details supporting the analyses described in the main text are discussed in the appendices A, B, C, E, D and F.

2 CFT with spacetime dependent velocities

In this section we focus on some universal algebraic features of CFT in the two-dimensional Minkowski spacetime which hold in any representation.

2.1 Commutation relations

Consider the chiral field algebras $\mathcal{A}_\pm = \{T_\pm(u), \phi_\pm(u), j_\pm(u), \dots ; u \in \mathbb{R}\}$ generating the right $(+)$ and left $(-)$ sectors of a CFT with U(1) symmetry. The algebraic properties defining the theory are encoded in commutation relations involving the following chiral field [22–25]:

(i) the chiral components of the energy-momentum tensor $T_\pm$, that satisfy

$$\big[\, T_\pm(u)\,, T_\pm(v)\,\big] = \mp \mathrm{i}\,\delta(u-v)\,\partial_v T_\pm(v) \pm 2\mathrm{i}\,\delta'(u-v)\,T_\pm(v) \mp \mathrm{i}\,\frac{c}{24\pi}\,\delta'''(u-v) \tag{2.1}$$

where c is the central charge of the CFT model;

(ii) the complex primary fields $\phi_\pm$, with dimensions $h_\pm$, occurring into

$$\big[\, T_\pm(u)\,, \phi_\pm(v)\,\big] = \mp \mathrm{i}\,\delta(u-v)\,\partial_v \phi_\pm(v) \pm \mathrm{i}\,h_\pm\,\delta'(u-v)\,\phi_\pm(v) \tag{2.2}$$

$$\big[\, T_\pm(u)\,, \phi^*_\pm(v)\,\big] = \mp \mathrm{i}\,\delta(u-v)\;\partial_v \phi^*_\pm(v) \pm \mathrm{i}\,h_\pm\delta'(u-v)\,\phi^*_\pm(v) \tag{2.3}$$

which are consistent[1] with (2.1).

(iii) the chiral components of a conserved current $j_\pm$, with dimension $h_{j_\pm} = 1$, which generate the U(1) transformations and satisfy

$$\big[\, j_\pm(u)\,, \phi_\pm(v)\,\big] = -\,\delta(u-v)\,\phi_\pm(v) \qquad\qquad \big[\, j_\pm(u)\,,\, \phi^*_\pm(v)\,\big] = \delta(u-v)\,\phi^*_\pm(v)\,. \tag{2.4}$$

The commutators (2.4) imply that the charge of ϕ and ϕ^* are equal to -1 and 1 respectively. Moreover,

$$\big[\, j_\pm(u)\,,\, j_\pm(v)\,\big] = \mp \mathrm{i}\,\frac{\kappa}{2\pi}\,\delta'(u-v) \tag{2.5}$$

where κ is a real constant and the r.h.s. is known as Schwinger term.

In the appendix A we report some consistency checks for the commutators (2.1) and (2.5) through the two-point functions in the fundamental representation which determines the normalization of the two-point functions for $j_\pm$ and $T_\pm$.

In order to obtain a conventional quantum field theory structure from the above algebraic setting, one should fix a Hilbert space representation $\mathcal{H}_+$ and $\mathcal{H}_-$ of the chiral algebras $\mathcal{A}_+$ and $\mathcal{A}_-$ respectively. After smearing with smooth test functions, the elements of $\mathcal{A}_\pm$ act as operators in $\mathcal{H}_+ \otimes \mathcal{H}_-$, that represents the physical state space of the system. Before fixing $\mathcal{H}_\pm$, in the following we employ (2.1)–(2.5) to obtain some results which are independent of the representation.

[1] For instance, the Jacobi identity involving (2.1) and (2.2) holds.

JHEP08(2025)021

2.2 Evolution through spacetime dependent velocities

In the following we consider a general setting where the temporal evolution of the right and the left sectors of the CFT is characterised by two independent velocities $V_\pm(u_\pm)$, which are smooth real functions depending on the light-cone coordinates $u_\pm \equiv x \pm t$. In particular, we focus on the Hamiltonian

$$H = \int_{-\infty}^{\infty} V_+(u_+)\, \mathcal{T}_+(u_+)\, \mathrm{d}u_+ + \int_{-\infty}^{\infty} V_-(u_-)\, \mathcal{T}_-(u_-)\, \mathrm{d}u_- \tag{2.6}$$

where

$$\mathcal{T}_\pm(u) \equiv T_\pm(u) - \mu_\pm\, j_\pm(u) \tag{2.7}$$

being $\mu_\pm$ defined as the chemical potentials associated to the two chiralities. The temporal evolution in the physical t generated by (2.6) with $\mu_+ = \mu_- = 0$ and strictly positive velocity $V_+ = V_-$ has been studied also in [26].

The evolution of the primary fields $\phi_\pm(u)$ generated by (2.6) is

$$\phi_\pm(\tau, u) \equiv \mathrm{e}^{\mathrm{i}\tau H}\, \phi_\pm(u)\, \mathrm{e}^{-\mathrm{i}\tau H} \tag{2.8}$$

where τ will be called modular time to highlight its different role with respect to the physical time t. Notice that the dimension of $V_\pm$ determines the dimension of τ. Furthermore, we remark that adding a real constant in the r.h.s. of (2.6) does not influence the corresponding evolution (2.8).

Taking the derivative of (2.8) with respect to τ provides the corresponding equation of motion

$$\partial_\tau \phi_\pm(\tau, u) = \mathrm{i}\,[\, H, \phi_\pm(\tau, u)\,] = \mathrm{i}\,[\, H\,, \mathrm{e}^{\mathrm{i}\tau H}\, \phi_\pm(u)\, \mathrm{e}^{-\mathrm{i}\tau H}\,] = \mathrm{i}\, \mathrm{e}^{\mathrm{i}\tau H}\,[\, H\,, \phi_\pm(u)\,]\, \mathrm{e}^{-\mathrm{i}\tau H}\,. \tag{2.9}$$

By using (2.2), the first commutator in (2.4) and (2.6), for finite values of u one finds

$$\begin{aligned} \partial_\tau \phi_\pm(\tau, u) &= \mathrm{e}^{\mathrm{i}\tau H} \int_{-\infty}^{\infty} V_\pm(v) \Big\{ \delta(v-u)\, (\pm\, \partial_u + \mathrm{i}\mu_\pm) \phi_\pm(u) \mp h_\pm\, \partial_v \delta(v-u) \phi_\pm(u) \Big\}\, \mathrm{d}v\, \mathrm{e}^{-\mathrm{i}\tau H} \\ &= \mathrm{e}^{\mathrm{i}\tau H} \Big\{ \pm\, V_\pm(u) (\partial_u \pm \mathrm{i}\mu_\pm) \phi_\pm(u) \pm h_\pm [\partial_u V_\pm(u)] \phi_\pm(u) \Big\}\, \mathrm{e}^{-\mathrm{i}\tau H} \end{aligned} \tag{2.10}$$

which leads to

$$\partial_\tau \phi_\pm(\tau, u) = \pm\, V_\pm(u) (\partial_u \pm \mathrm{i}\mu_\pm) \phi_\pm(\tau, u) \pm h_\pm [\partial_u V_\pm(u)] \phi_\pm(\tau, u)\,. \tag{2.11}$$

In order to solve (2.11), let us consider the following linear first order equation

$$\partial_\tau \xi_\pm(\tau, u) = \pm\, V_\pm(u)\, \partial_u \xi_\pm(\tau, u) \tag{2.12}$$

with initial condition

$$\xi_\pm(0, u) = u\,. \tag{2.13}$$

We assume that $V_\pm(u)$ are smooth functions with a finite number of zeros; hence they are finite functions for any finite value of u. We introduce $w_\pm(u)$ through the following condition

$$w'_\pm(u) = \frac{1}{V_\pm(u)} \tag{2.14}$$

JHEP08(2025)021

and consider the interval $A \equiv [a, b]$ identified by two consecutive zeros of $V_\pm(u)$, i.e.

$$V_\pm(a) = V_\pm(b) = 0\,. \tag{2.15}$$

When $u \in A$, the function $w_\pm(u)$ is monotonic and therefore its inverse function $w_\pm^{-1}(u)$ is well defined. In this case, we define

$$\xi_\pm(\tau, u) \equiv w_\pm^{-1}(w_\pm(u) \pm \tau)\,. \tag{2.16}$$

The functions $\xi_\pm(\tau, u)$ satisfy the initial condition (2.13) and

$$\partial_\tau \xi_\pm(\tau, u) = \pm\, V_\pm(\xi_\pm(\tau, u)) \qquad\qquad \partial_u \xi_\pm(\tau, u) = \frac{V_\pm(\xi_\pm(\tau, u))}{V_\pm(u)}\,. \tag{2.17}$$

The solution of the equation of motion (2.11) is

$$\phi_\pm(\tau, u) = \mathrm{e}^{\pm \mathrm{i}\mu_\pm[\xi_\pm(\tau,u)-u]}\, [\partial_u \xi_\pm(\tau, u)]^{h_\pm}\, \phi_\pm(\xi_\pm(\tau, u)) \tag{2.18}$$

and satisfies the initial condition

$$\phi_\pm(0, u) = \phi_\pm(u)\,. \tag{2.19}$$

Analogously, the evolution of the primary fields $\phi_\pm^*$ is described by

$$\phi_\pm^*(\tau, u) = \mathrm{e}^{\mp \mathrm{i}\mu_\pm[\xi_\pm(\tau,u)-u]}\, [\partial_u \xi_\pm(\tau, u)]^{h_\pm}\, \phi_\pm^*(\xi_\pm(\tau, u))\,. \tag{2.20}$$

The above considerations can be applied to explore also the evolution of the chiral currents generated by (2.6), namely $j_\pm(\tau, u) \equiv \mathrm{e}^{\mathrm{i}\tau H}\, j_\pm(u)\, \mathrm{e}^{-\mathrm{i}\tau H}$. The corresponding equation of motion is affected by the Schwinger term in (2.5) and has the form

$$\partial_\tau j_\pm(\tau, u) = \pm\, V_\pm(u)\, \partial_u j_\pm(\tau, u) \pm [\partial_u V_\pm(u)] j_\pm(\tau, u) \pm \frac{\kappa\mu_\pm}{2\pi}\, \partial_u V_\pm(u) \tag{2.21}$$

$$= \pm\, \partial_u [V_\pm(u)\, j_\pm(\tau, u)] \pm \frac{\kappa\mu_\pm}{2\pi}\, \partial_u V_\pm(u) \tag{2.22}$$

with initial condition $j_\pm(0, u) = j_\pm(u)$; whose solution is

$$j_\pm(\tau, u) = [\partial_u \xi_\pm(\tau, u)]\, j_\pm(\xi_\pm(\tau, u)) - \frac{\kappa\mu_\pm}{2\pi}\, [1 - \partial_u \xi_\pm(\tau, u)]\,. \tag{2.23}$$

The continuity equation (2.22) can be written also as

$$\partial_\tau j_\pm(\tau, u) = \pm\, \partial_u \left[V_\pm(u) \left(j_\pm(\tau, u) + \frac{\kappa\mu_\pm}{2\pi} \right) \right] \tag{2.24}$$

or, equivalently, as

$$\partial_\tau \left(j_\pm(\tau, u) + \frac{\kappa\mu_\pm}{2\pi} \right) = \pm\, \partial_u \left[V_\pm(u) \left(j_\pm(\tau, u) + \frac{\kappa\mu_\pm}{2\pi} \right) \right]. \tag{2.25}$$

In the representations investigated in this manuscript, the mean value of $j_\pm(\tau, u) + \frac{\kappa\mu_\pm}{2\pi}$ vanishes (see (4.1) and (6.1), with the velocities given by (4.7) and (6.9) respectively). The previous observation leads us to realise that (2.22) is equivalent to

$$\partial_\tau \left(j_\pm(\tau, u) + \tilde{\alpha}_\pm \frac{\kappa\mu_\pm}{2\pi} \right) = \pm\, \partial_u \left[V_\pm(u) \left(j_\pm(\tau, u) + \alpha_\pm \frac{\kappa\mu_\pm}{2\pi} \right) \right] \pm (1 - \alpha_\pm) \frac{\kappa\mu_\pm}{2\pi}\, \partial_u V_\pm(u) \tag{2.26}$$

JHEP08(2025)021

where $\alpha_\pm$ and $\tilde{\alpha}_\pm$ are real constants. However, in our analyses we mainly consider the case where $\alpha_\pm = \tilde{\alpha}_\pm = 0$, as discussed in section 3.1.

The evolution of $T_\pm(u)$ generated by (2.6), i.e. $T_\pm(\tau, u) \equiv \mathrm{e}^{\mathrm{i}\tau H}\, T_\pm(u)\, \mathrm{e}^{-\mathrm{i}\tau H}$, can be explored by employing (2.1), (2.2) and (2.5), which lead to[2]

$$\partial_\tau T_\pm(\tau,u) = \pm\, V_\pm(u)\, \partial_u T_\pm(\tau,u) \pm 2\big[\partial_u V_\pm(u)\big] T_\pm(\tau,u) \mp \frac{c}{24\pi}\, \partial_u^3 V_\pm(u) \mp \mu_\pm V_\pm(u)\, \partial_u j_\pm(\tau,u) \tag{2.29}$$

where $j_\pm(\tau, u)$ is given by (2.23). The occurrence of $j_\pm(\tau, u)$ in (2.29) leads us to consider the evolution of $\mathcal{T}_\pm(u)$, namely $\mathcal{T}_\pm(t, x) \equiv \mathrm{e}^{\mathrm{i}tH}\, \mathcal{T}_\pm(x)\, \mathrm{e}^{-\mathrm{i}tH}$. Indeed, the equation of motion for these fields reads

$$\partial_\tau \mathcal{T}_\pm(\tau,u) = \pm\, V_\pm(u) \partial_u \mathcal{T}_\pm(\tau,u) \pm 2\big[\partial_u V_\pm(u)\big] \mathcal{T}_\pm(\tau,u) \mp \frac{\kappa\mu_\pm^2}{2\pi}\, \partial_u V_\pm(u) \mp \frac{c}{24\pi}\, \partial_u^3 V_\pm(u) \tag{2.30}$$

with the initial condition $\mathcal{T}_\pm(0, u) = \mathcal{T}_\pm(u)$, where only the field $\mathcal{T}_\pm(\tau, u)$ occurs.

Multiplying both sides of (2.30) by $V_\pm(u)$, we obtain the following equivalent form

$$\partial_\tau \big[V_\pm(u)\, \mathcal{T}_\pm(\tau,u)\big] = \pm\, \partial_u \big[V_\pm(u)^2\, \mathcal{T}_\pm(\tau,u)\big] \mp \frac{\kappa\mu_\pm^2}{4\pi}\, \partial_u V_\pm(u)^2 \mp \frac{c}{24\pi}\, V_\pm(u)\, \partial_u^3 V_\pm(u)\,. \tag{2.31}$$

This differential equation can be arranged as

$$\partial_\tau \left[V_\pm(u) \left(\mathcal{T}_\pm(\tau,u) - \frac{\kappa\mu_\pm^2}{4\pi} \right) \right] = \pm\, \partial_u \left[V_\pm(u)^2 \left(\mathcal{T}_\pm(\tau,u) - \frac{\kappa\mu_\pm^2}{4\pi} \right) \right] \mp \frac{c}{24\pi}\, V_\pm(u)\, \partial_u^3 V_\pm(u)\,. \tag{2.32}$$

As done in (2.26) for the differential equation for $j_\pm(\tau, u)$, (2.32) can be written also in a general form involving the constants $\alpha_\pm$ and $\tilde{\alpha}_\pm$ that we do not find worth reporting here.

In the finite density representation on the line, where the mean values (4.1) and the velocity $V_\pm(u) = V(u)$ in (4.7) must be used, the operators $\mathcal{T}_\pm(\tau, u) - \frac{\kappa\mu_\pm^2}{4\pi}$ have vanishing mean values and $\partial_u^3 V(u) = 0$. Instead, in the finite density representation on the circle of length L, where the mean values (6.1) and the velocity $V_\pm(u) = V_L(u)$ in (6.9) must be employed, it is more convenient to write (2.32) as follows

$$\begin{aligned} \partial_\tau \left[V_\pm(u) \left(\mathcal{T}_\pm(\tau,u) - \frac{\kappa\mu_\pm^2}{4\pi} + \frac{\pi c}{12L^2} \right) \right] &= \pm \partial_u \left[V_\pm(u)^2 \left(\mathcal{T}_\pm(\tau,u) - \frac{\kappa\mu_\pm^2}{4\pi} + \frac{\pi c}{12L^2} \right) \right] \\ &\quad \mp \frac{c}{24\pi} \left(\frac{2\pi^2}{L^2} \partial_u V_\pm(u)^2 + V_\pm(u) \partial_u^3 V_\pm(u) \right). \end{aligned} \tag{2.33}$$

Indeed, in this representation the operators within the round brackets in (2.33) have vanishing mean values and $\frac{2\pi^2}{L^2}\, \partial_u V_L(u)^2 + V_L(u)\, \partial_u^3 V_L(u) = 0$ for the velocity (6.9).

[2]The evolution in the physical time t is generated by (2.6) with constant velocities $V_\pm$ and $\mu_\pm = 0$. In this case, from (2.1), one finds

$$\partial_t T_\pm(t,u) = \pm V_\pm\, \partial_u T_\pm(t,u) \tag{2.27}$$

whose solution is

$$T_\pm(t,u) = T_\pm(u \pm V_\pm t) \tag{2.28}$$

We choose the convention where $V_\pm = 1$.

JHEP08(2025)021

The solution of (2.30) reads

$$\mathcal{T}_{\pm}(\tau,u) = \big[\partial_u \xi_{\pm}(\tau,u)\big]^2\, \mathcal{T}_{\pm}(\xi_{\pm}(\tau,u)) + \frac{\kappa\mu_{\pm}^2}{4\pi}\Big\{1-\big[\partial_u \xi_{\pm}(\tau,u)\big]^2\Big\} - \frac{c}{24\pi}\,\mathcal{S}_u[\xi_{\pm}](\tau,u) \quad (2.34)$$

where $\mathcal{S}_u[\xi](\tau,u)$ is the Schwarzian derivative of the functions $\xi_{\pm}(\tau,u)$, i.e.

$$\mathcal{S}_u[\xi](\tau,u) = \frac{\partial_u^3 \xi(\tau,u)}{\partial_u \xi(\tau,u)} - \frac{3}{2}\left[\frac{\partial_u^2 \xi(\tau,u)}{\partial_u \xi(\tau,u)}\right]^2 . \quad (2.35)$$

The solution (2.34) has been found by exploiting the following identity

$$\partial_\tau \mathcal{S}_u[\xi_{\pm}](\tau,u) = \pm\, V_{\pm}(u)\, \partial_u \mathcal{S}_u[\xi_{\pm}](\tau,u) \pm 2\big[\partial_u V_{\pm}(u)\big]\mathcal{S}_u[\xi_{\pm}](\tau,u) \pm \partial_u^3 V_{\pm}(u) \quad (2.36)$$

which is a consequence of (2.12) and (2.35). Multiplying (2.36) by $V_{\pm}(u)$, it can be written as

$$\partial_\tau\big\{V_{\pm}(u)\,\mathcal{S}_u[\xi_{\pm}](\tau,u)\big\} = \pm\,\partial_u\big\{V_{\pm}(u)^2\,\mathcal{S}_u[\xi_{\pm}](\tau,u)\big\} \pm V_{\pm}(u)\,\partial_u^3 V_{\pm}(u)\,. \quad (2.37)$$

By employing the second expression in (2.17), one finds that (2.35) can be expressed as follows

$$\begin{aligned}\mathcal{S}_u[\xi_{\pm}](\tau,u) \,=\, & \frac{V_{\pm}(\xi(\tau,u))^2}{V_{\pm}(u)^2}\left[\frac{\partial_u^2 V_{\pm}(\xi(\tau,u))}{V_{\pm}(\xi(\tau,u))} - \frac{1}{2}\left(\frac{\partial_u V_{\pm}(\xi(\tau,u))}{V_{\pm}(\xi(\tau,u))}\right)^2\right] \\ & - \left[\frac{\partial_u^2 V_{\pm}(u)}{V_{\pm}(u)} - \frac{1}{2}\left(\frac{\partial_u V_{\pm}(u)}{V_{\pm}(u)}\right)^2\right].\end{aligned} \quad (2.38)$$

This result will be applied in section 4.2 and section 6.2 for specific expressions of $V_{\pm}(u)$.

3 Conservation laws, currents and charges

In this section we discuss the conservation of some charges in the spacetime diamond

$$\mathcal{D}_A \equiv \big\{(x,t) : a \leqslant u_+ \leqslant b\,,\ a \leqslant u_- \leqslant b\big\} \quad (3.1)$$

corresponding to the domain of dependence of the interval $A \equiv [a,b]$, which can be identified by two consecutive zeros $a < b$ of $V_{\pm}(u)$. The spacetime coordinates (x,t) of the vertices of $\mathcal{D}_A$ are $P_a = (a,0)$, $P_b = (b,0)$, $P_{+\infty} = (\frac{a+b}{2}, \frac{b-a}{2})$ and $P_{-\infty} = (\frac{a+b}{2}, -\frac{b-a}{2})$. The function (2.16) provides $\xi_{\pm}(\tau,u_{\pm})$, which allow to construct the trajectory in $\mathcal{D}_A$ parameterised by $\tau \in \mathbb{R}$ whose generic point has spacetime coordinates

$$x(\tau) = \frac{\xi_+(\tau,u_+) + \xi_-(\tau,u_-)}{2} \qquad t(\tau) = \frac{\xi_+(\tau,u_+) - \xi_-(\tau,u_-)}{2} \quad (3.2)$$

where (u_+,u_-) are the light-cone coordinates of the initial point corresponding to $\tau = 0$.

3.1 Electric charge and helicity

From the commutation relations (2.4), the electric charge density at $\tau = 0$ is

$$\varrho(\tau=0;x,t) \equiv j_+(u_+) + j_-(u_-) \quad (3.3)$$

JHEP08(2025)021

where $u_\pm = x \pm t$ are the light-cone coordinates. Hence, its modular evolution reads

$$\varrho(\tau; x, t) \equiv j_+(\tau, u_+) + j_-(\tau, u_-) \tag{3.4}$$

where $j_\pm(\tau, u_\pm)$ are given by (2.23).

We remark that the quantity (3.4) and all the subsequent ones defined in a similar way depend both on the physical time t associated to the Hamiltonian of the CFT and on the evolution parameter τ associated to the Hamiltonian (2.6), which will play the role of the modular Hamiltonian from the next section.

By using (2.21) and $\partial_x = \partial_{u_+} + \partial_{u_-}$, for $\mu_\pm = 0$ we find the continuity relation

$$\partial_\tau \varrho(\tau; x, t) = -\,\partial_x j_x(\tau; x, t) \tag{3.5}$$

where

$$j_x(\tau; x, t) \equiv -\,V_+(u_+)\, j_+(\tau, u_+) + V_-(u_-)\, j_-(\tau, u_-) \tag{3.6}$$

defines the space component of the electric current when spacetime dependent velocities $V_\pm(u_\pm)$ occur. In the special case of $V_+(u_+) = V_-(u_-) = 1$ identically and for $\tau = 0$, from (2.23) we find that the current (3.6) becomes

$$j_x(\tau = 0; x, t)\big|_{V_+ = V_- = 1} = -\,j_+(u_+) + j_-(u_-) \tag{3.7}$$

i.e. the standard CFT expressions employed e.g. in [13–16], which has vanishing expectation value in the fundamental representation.

When $\mu_\pm \neq 0$, the Schwinger term in (2.5) generates an additional contribution with respect to (3.5). In the case we are exploring, given the definition (3.6), by employing (2.21) and $\partial_t = \partial_{u_+} - \partial_{u_-}$ we find the following continuity equation

$$\partial_\tau \varrho(\tau; x, t) = -\,\partial_x j_x(\tau; x, t) + \frac{\kappa}{2\pi}\,\partial_t\big[\,\mu_+\, V_+(u_+) + \mu_-\, V_-(u_-)\,\big] \tag{3.8}$$

which naturally leads us to introduce the following t-component for the charge current

$$j_t(\tau; x, t) \equiv \frac{\kappa}{2\pi}\,\big[\,\mu_+\, V_+(u_+) + \mu_-\, V_-(u_-)\,\big] \tag{3.9}$$

which is independent of τ.

We emphasize that, from either (2.21) or (2.24) and $\partial_x = \partial_{u_+} + \partial_{u_-}$, it is straightforward to observe that (3.8) can be written also as

$$\partial_\tau \varrho(\tau; x, t) = -\,\partial_x j_x(\tau; x, t) + \frac{\kappa}{2\pi}\,\partial_x\big[\,\mu_+\, V_+(u_+) - \mu_-\, V_-(u_-)\,\big] \tag{3.10}$$

$$= -\,\partial_x \left(j_x(\tau; x, t) - \frac{\kappa}{2\pi}\,\big[\,\mu_+\, V_+(u_+) - \mu_-\, V_-(u_-)\,\big] \right). \tag{3.11}$$

This observation, or (2.25), leads us to introduce instead the operators

$$\hat{\varrho}(\tau; x, t) \equiv \left(j_+(\tau, u_+) + \frac{\kappa\mu_+}{2\pi} \right) + \left(j_-(\tau, u_-) + \frac{\kappa\mu_-}{2\pi} \right) \tag{3.12}$$

and

$$\hat{j}_x(\tau; x, t) \equiv -\,V_+(u_+) \left(j_+(\tau, u_+) + \frac{\kappa\mu_+}{2\pi} \right) + V_-(u_-) \left(j_-(\tau, u_-) + \frac{\kappa\mu_-}{2\pi} \right) \tag{3.13}$$

JHEP08(2025)021

which satisfy the following continuity equation also when $\mu_\pm \neq 0$

$$\partial_\tau \hat{\varrho}(\tau; x, t) = -\,\partial_x \hat{j}_x(\tau; x, t)\,. \tag{3.14}$$

In section 4.1 we will see that the operators (3.12) and (3.13) have vanishing mean values in the finite density representation; hence they do not provide the operators employed in [13–16] when $\tau = 0$ and $V_+(u_+) = V_-(u_-) = 1$ identically. Thus, in our analysis we mainly adopt the definitions (3.4) and (3.6).

In the following, also for the helicity, the energy and the momentum we can introduce operators having vanishing mean values in the finite density representation and playing the same role of (3.12) and (3.13). The above considerations are straightforwardly adapted to these operators.

By employing (3.9), the continuity relation (3.8) takes the form

$$\partial_\tau \varrho(\tau; x, t) = -\,\partial_x j_x(\tau; x, t) + \partial_t j_t(\tau; x, t) \tag{3.15}$$

which can be rewritten also in following covariant form

$$\partial_\tau \varrho(\tau; x, t) = \partial_\mu j^\mu(\tau; x, t) \tag{3.16}$$

via the Minkowski metric $\eta_{\mu\nu} \equiv \mathrm{diag}(1, -1)$ in the spacetime parameterised by $x^\mu = (t, x)$, that allows to raise the index of the vector $j_\mu \equiv (j_t, j_x)$, finding $j^\mu \equiv (j_t, -j_x)$.

We remark that the arbitrary additive constant shifts in (3.6) and (3.9) can be fixed also by requiring the vanishing of these quantities at the vertices P_a, P_b, $P_{+\infty}$ and $P_{-\infty}$ of the spacetime diamond $\mathcal{D}_A$ in (3.1), i.e. for $u_\pm \in \{a, b\}$.

From (3.4), we can define the total electric charge in $\mathcal{D}_A$ as

$$Q_A \equiv \int_{\mathcal{D}_A} \varrho(\tau; x, t)\, \mathrm{d}x\, \mathrm{d}t = \frac{b-a}{2} \left(\int_a^b j_+(\tau, u_+)\, \mathrm{d}u_+ + \int_a^b j_-(\tau, u_-)\, \mathrm{d}u_- \right) \tag{3.17}$$

which is independent of x and t by construction. The independence of τ in (3.17), i.e. the condition $\partial_\tau Q_A = 0$ corresponding to the conservation of Q_A in $\mathcal{D}_A$, follows from the equations of motion for the currents in (2.21) combined with (2.15).

From (3.6) and (3.9), notice that $\partial_\tau j_x$ is non vanishing, while $\partial_\tau j_t = 0$, being j_t independent of τ. In particular, by employing (2.22) we obtain

$$\begin{aligned} \partial_\tau j_x(\tau; x, t) \,=\, & -\,\partial_{u_+}\big[\, V_+(u_+)^2\, j_+(\tau, u_+)\,\big] - \partial_{u_-}\big[\, V_-(u_-)^2\, j_+(\tau, u_-)\,\big] \\ & + \frac{\partial_{u_+} V_+(u_+)^2}{2}\, j_+(\tau, u_+) + \frac{\partial_{u_-} V_-(u_-)^2}{2}\, j_-(\tau, u_-) \\ & - \frac{\kappa}{4\pi}\Big[\, \mu_+\, \partial_{u_+} V_+(u_+)^2 + \mu_-\, \partial_{u_-} V_-(u_-)^2 \,\Big] \end{aligned} \tag{3.18}$$

which implies that $j_x(\tau; x, t)$ does not correspond to the density of a conserved quantity in the diamond $\mathcal{D}_A$. This happens because of the terms in the second line of (3.18); indeed the first line and the third line can be written as total derivatives e.g. in x and t respectively.

The helicity can be investigated in a similar way. Since ϕ_+ and ϕ_- have opposite helicities, the commutators (2.4) lead us to introduce the following density

$$\chi(\tau; x, t) \equiv j_+(\tau, u_+) - j_-(\tau, u_-)\,. \tag{3.19}$$

JHEP08(2025)021

From (2.21), we find the continuity relation

$$\partial_\tau \chi(\tau;x,t) = \partial_t k_t(\tau;x,t) - \partial_x k_x(\tau;x,t) = \partial_\mu k^\mu(\tau;x,t) \tag{3.20}$$

where the components of the helicity current are defined as

$$k_x(\tau;x,t) \equiv -V_+(u_+)\, j_+(\tau,u_+) - V_-(u_-)\, j_-(\tau,u_-) \tag{3.21}$$

$$k_t(\tau;x,t) \equiv \frac{\kappa}{2\pi}\left[\,\mu_+\, V_+(u_+) - \mu_-\, V_-(u_-)\,\right] \tag{3.22}$$

which vanish for $u_\pm \in \{a,b\}$. The helicity charge in $\mathcal{D}_A$ following from (3.19) is

$$\widetilde{Q}_A \equiv \int_{\mathcal{D}_A} \chi(\tau;x,t)\,\mathrm{d}x\,\mathrm{d}t = \frac{b-a}{2}\left(\int_a^b j_+(\tau,u_+)\,\mathrm{d}u_+ - \int_a^b j_-(\tau,u_-)\,\mathrm{d}u_-\right). \tag{3.23}$$

This quantity is independent of x, t and also conserved, i.e. independent of τ, as we can find from (2.21) and (2.15).

3.2 Energy and momentum

The energy density can be introduced from (2.6) as follows

$$\mathcal{E}(\tau;x,t) \equiv V_+(u_+)\,\mathcal{T}_+(\tau,u_+) + V_-(u_-)\,\mathcal{T}_-(\tau,u_-) + f_+(u_+) + f_-(u_-) \tag{3.24}$$

and $f_\pm(u_\pm)$ are real functions that can be exploited to fix the mean value of this operator but they do not influence the following analysis because they are independent of τ.

The equations of motion (2.30) lead to

$$\begin{aligned}\partial_\tau \mathcal{E}(\tau;x,t) = {}& \partial_{u_+}\left[\,V_+(u_+)^2\,\mathcal{T}_+(\tau,u_+)\,\right] - \frac{\kappa\,\mu_+^2}{2\pi}\,\partial_{u_+}\left[V_+(u_+)^2\right] - \frac{c}{24\pi}\,V_+(u_+)\,\partial_{u_+}^3 V_+(u_+) \\ & - \partial_{u_-}\left[\,V_-(u_-)^2\,\mathcal{T}_-(\tau,u_-)\,\right] + \frac{\kappa\,\mu_-^2}{2\pi}\,\partial_{u_-}\left[V_-(u_-)^2\right] + \frac{c}{24\pi}\,V_-(u_-)\,\partial_{u_-}^3 V_-(u_-)\,.\end{aligned} \tag{3.25}$$

By using the following identity

$$\partial_u\left(V(u)^2\,\mathcal{V}[V](u)\right) = V(u)\,\partial_u^3 V(u) \tag{3.26}$$

where

$$\mathcal{V}[V](u) \equiv \frac{V''(u)}{V(u)} - \frac{1}{2}\left[\frac{V'(u)}{V(u)}\right]^2 \tag{3.27}$$

and the fact that $\partial_x = \partial_{u_+} + \partial_{u_-}$ and $\partial_t = \partial_{u_+} - \partial_{u_-}$, the differential equation (3.25) can be written also in the form of the continuity relation

$$\partial_\tau \mathcal{E}(\tau;x,t) = \partial_t \mathcal{J}_t(\tau;x,t) - \partial_x \mathcal{J}_x(\tau;x,t) = \partial_\mu \mathcal{J}^\mu(\tau;x,t) \tag{3.28}$$

where

$$\mathcal{J}_x(\tau;x,t) \equiv -V_+(u_+)^2\,\mathcal{T}_+(\tau,u_+) + V_-(u_-)^2\,\mathcal{T}_-(\tau,u_-) \tag{3.29}$$

$$\begin{aligned}\mathcal{J}_t(\tau;x,t) \equiv {}& -\frac{\kappa}{4\pi}\left\{\mu_+^2\,V_+(u_+)^2 + \mu_-^2\,V_-(u_-)^2\right\} \\ & - \frac{c}{24\pi}\left\{V_+(u_+)^2\,\mathcal{V}[V_+](u_+) + V_-(u_-)^2\,\mathcal{V}[V_-](u_-)\right\} + C_{\mathcal{J}}\,.\end{aligned} \tag{3.30}$$

JHEP08(2025)021

We remark that (3.29) satisfies

$$\mathcal{J}_x(\tau=0;x,t)\big|_{V_+=V_-=1} = -\,\mathcal{T}_+(u_+) + \mathcal{T}_-(u_-) \tag{3.31}$$

whose expectation value in the finite density representation (see (4.1)) agrees with the corresponding result found in [15] at zero temperature. In (3.30) we have introduced the constant $C_{\mathcal{J}}$ because, while $\mathcal{J}_x$ vanishes for $u_\pm \in \{a,b\}$, this condition is not guaranteed for $\mathcal{J}_t$.

The energy density (3.24) leads us to define the total energy in $\mathcal{D}_A$ as follows

$$\begin{aligned} E_A &\equiv \int_{\mathcal{D}_A} \mathcal{E}(\tau;x,t)\,\mathrm{d}x\,\mathrm{d}t \\ &= \frac{b-a}{2}\left(\int_a^b \Big[V_+(u_+)\,\mathcal{T}_+(\tau,u_+) + f_+(u_+)\Big]\mathrm{d}u_+ + \int_a^b \Big[V_-(u_-)\,\mathcal{T}_-(\tau,u_-) + f_-(u_-)\Big]\mathrm{d}u_-\right) \end{aligned} \tag{3.32}$$

which is constant, i.e. independent of x, t and τ. Its conservation along the τ-evolution, i.e. the fact that $\partial_\tau E_A = 0$, is obtained from the continuity equation (3.25), the identity (3.26) and the condition (2.15).

By employing (2.31), from (3.30) and (3.29) we obtain respectively $\partial_\tau \mathcal{J}_t = 0$ and

$$\begin{aligned} \partial_\tau \mathcal{J}_x(\tau;x,t) \,=\, & -\,\partial_{u_+}\big[\,V_+(u_+)^3\,\mathcal{T}_+(\tau,u_+)\,\big] - \partial_{u_-}\big[\,V_-(u_-)^3\,\mathcal{T}_+(\tau,u_-)\,\big] \\ & + \frac{\partial_{u_+}V_+(u_+)^3}{3}\,\mathcal{T}_+(\tau,u_+) + \frac{\partial_{u_-}V_-(u_-)^3}{3}\,\mathcal{T}_-(\tau,u_-) \\ & + \frac{\kappa}{6\pi}\Big[\,\mu_+^2\,\partial_{u_+}V_+(u_+)^3 + \mu_-^2\,\partial_{u_-}V_-(u_-)^3\,\Big] + \frac{c}{24\pi}\Big[\,V_+(u_+)^2\,\partial_{u_+}^3 V_+(u_+) + V_-(u_-)^2\,\partial_{u_-}^3 V_-(u_-)\,\Big] \end{aligned} \tag{3.33}$$

which tells us that $\mathcal{J}_x(\tau;x,t)$ is not the density of a conserved quantity in the diamond.

We find it worth introducing also the following generalized momentum density

$$\widetilde{\mathcal{E}}(\tau;x,t) \equiv V_+(u_+)\,\mathcal{T}_+(\tau,u_+) - V_-(u_-)\,\mathcal{T}_-(\tau,u_-) + f_+(u_+) - f_-(u_-) \tag{3.34}$$

where for the real functions $f_\pm(u_\pm)$ we can repeat the considerations made below (3.24). The equations of motion (2.30) give

$$\begin{aligned} \partial_\tau \widetilde{\mathcal{E}}(\tau;x,t) \,=\, & \partial_{u_+}\big[\,V_+(u_+)^2\,\mathcal{T}_+(\tau,u_+)\,\big] - \frac{\kappa\mu_+^2}{2\pi}\,\partial_{u_+}\big[V_+(u_+)^2\big] - \frac{c}{24\pi}\,V_+(u_+)\,\partial_{u_+}^3 V_+(u_+) \\ & + \partial_{u_-}\big[\,V_-(u_-)^2\,\mathcal{T}_-(\tau,u_-)\,\big] - \frac{\kappa\mu_-^2}{2\pi}\,\partial_{u_-}\big[V_-(u_-)^2\big] - \frac{c}{24\pi}\,V_-(u_-)\,\partial_{u_-}^3 V_-(u_-) \end{aligned} \tag{3.35}$$

or, equivalently,

$$\partial_\tau \widetilde{\mathcal{E}}(\tau;x,t) = \partial_t \widetilde{\mathcal{J}}_t(\tau;x,t) - \partial_x \widetilde{\mathcal{J}}_x(\tau;x,t) = \partial_\mu \widetilde{\mathcal{J}}^\mu(\tau;x,t) \tag{3.36}$$

where

$$\widetilde{\mathcal{J}}_x(\tau;x,t) \equiv -\,V_+(u_+)^2\,\mathcal{T}_+(\tau,u_+) - V_-(u_-)^2\,\mathcal{T}_-(\tau,u_-) \tag{3.37}$$

$$\begin{aligned} \widetilde{\mathcal{J}}_t(\tau;x,t) \equiv & -\frac{\kappa}{4\pi}\Big\{\mu_+^2\,V_+(u_+)^2 - \mu_-^2\,V_-(u_-)^2\Big\} \\ & - \frac{c}{24\pi}\Big\{V_+(u_+)^2\,\mathcal{V}[V_+](u_+) - V_-(u_-)^2\,\mathcal{V}[V_-](u_-)\Big\} + C_{\widetilde{\mathcal{J}}}\,. \end{aligned} \tag{3.38}$$

JHEP08(2025)021

In analogy with (3.32), the momentum density (3.34) leads us to introduce the total momentum in $\mathcal{D}_A$ as follows

$$\widetilde{E}_A \equiv \int_{\mathcal{D}_A} \widetilde{\mathcal{E}}(\tau; x, t)\, \mathrm{d}x\, \mathrm{d}t \tag{3.39}$$
$$= \frac{b-a}{2} \left(\int_a^b \Big[V_+(u_+)\, \mathcal{T}_+(\tau, u_+) + f_+(u_+) \Big] \mathrm{d}u_+ - \int_a^b \Big[V_-(u_-)\, \mathcal{T}_-(\tau, u_-) + f_-(u_-) \Big] \mathrm{d}u_- \right)$$

which is independent of x, t and also of τ, as it can be found from the corresponding continuity equation (3.35), the identity (3.26) and the condition (2.15).

The application of the above analysis to the chiral primaries is discussed in the appendix B.

3.3 Transformation generated by the generalized momentum

The operator (3.34) provides the following evolution operator

$$P \equiv \int_{-\infty}^{\infty} \Big[V_+(u_+)\, \mathcal{T}_+(\tau, u_+) + f_+(u_+) \Big] \mathrm{d}u_+ - \int_{-\infty}^{\infty} \Big[V_-(u_-)\, \mathcal{T}_-(\tau, u_-) + f_-(u_-) \Big] \mathrm{d}u_- \,. \tag{3.40}$$

The evolution of a primary $\phi_\pm$ generated by (3.40) reads

$$\widetilde{\phi}_\pm(\lambda, u) \equiv \mathrm{e}^{\mathrm{i}\lambda P}\, \phi_\pm(u)\, \mathrm{e}^{-\mathrm{i}\lambda P} \tag{3.41}$$

and it can be studied by slightly modifying the analysis described for (2.8). This leads to the following equation for (3.41)

$$\partial_\lambda \widetilde{\phi}_\pm(\lambda, u) = V_\pm(u)(\partial_u \pm \mathrm{i}\mu_\pm)\widetilde{\phi}_\pm(\lambda, u) + h_\pm \big[\partial_u V_\pm(u)\big] \widetilde{\phi}_\pm(\lambda, u) \tag{3.42}$$

with initial condition $\widetilde{\phi}_\pm(0, u) = \phi_\pm(u)$, which can be solved through $\zeta_\pm(\lambda, x)$ satisfying

$$\partial_\lambda \zeta_\pm(\lambda, u) = V_\pm(u)\, \partial_u \zeta_\pm(\lambda, u) \tag{3.43}$$

with the initial condition

$$\zeta_\pm(0, u) = u \,. \tag{3.44}$$

which can be compared with the differential equation (2.12) and its initial condition (2.13) respectively. The solution of (3.43) and (3.44) can expressed for $u \in [a, b]$ between two consecutive zeros of $V_\pm$ in terms of (2.14) as follows

$$\zeta_\pm(\lambda, u) \equiv w_\pm^{-1}\big(w_\pm(u) + \lambda\big) \tag{3.45}$$

which is slightly different from (2.16). The expressions (3.45) satisfy

$$\partial_\lambda \zeta_\pm(\lambda, u) = V_\pm(\zeta_\pm(\lambda, u)) \qquad \partial_u \zeta_\pm(\lambda, u) = \frac{V_\pm(\zeta_\pm(\lambda, u))}{V_\pm(u)} \,. \tag{3.46}$$

Comparing the functions in (3.45) with the ones in (2.16), we observe that $\zeta_+(\lambda, u) = \xi_+(\lambda, u)$, while $\zeta_-(\lambda, u) = \xi_-(-\lambda, u)$. The infinitesimal transformation is obtained by expanding (3.45) for small λ and this gives (see also the remark 4.2 of [26])

$$\zeta_\pm(\lambda, u) = u + V_\pm(u)\, \lambda + O(\lambda^2) \,. \tag{3.47}$$

For constant velocities $V_\pm$, we have $\zeta_\pm(\lambda, u) = u + V_\pm \lambda$ for (3.45), i.e. the spatial translations.

JHEP08(2025)021

By using (3.45), for the evolution (3.41) we find

$$\widetilde{\phi}_{\pm}(\lambda,u) = \mathrm{e}^{\pm \mathrm{i}\mu_{\pm}[\zeta_{\pm}(\lambda,u)-u]} \left[\partial_u \zeta_{\pm}(\lambda,u)\right]^{h_{\pm}} \phi_{\pm}(\zeta_{\pm}(\lambda,u)) \tag{3.48}$$

which satisfies the initial condition $\widetilde{\phi}_{\pm}(0,u) = \phi_{\pm}(u)$, as expected. Notice that the r.h.s.'s of (2.18) and (3.48) are formally identical. Thus, as for the evolutions in λ of $j_{\pm}$ and of $\mathcal{T}_{\pm}$, i.e.

$$\widetilde{j}_{\pm}(\lambda,u) \equiv \mathrm{e}^{\mathrm{i}\lambda\widetilde{H}}\, j_{\pm}(u)\, \mathrm{e}^{-\mathrm{i}\lambda\widetilde{H}} \qquad\qquad \widetilde{\mathcal{T}}_{\pm}(\lambda,u) \equiv \mathrm{e}^{\mathrm{i}\lambda\widetilde{H}}\, \mathcal{T}_{\pm}(u)\, \mathrm{e}^{-\mathrm{i}\lambda\widetilde{H}} \tag{3.49}$$

we find that they are given by the r.h.s.'s of (2.23) and (2.34) respectively, with $\xi_{\pm}(\tau,u)$ replaced by $\zeta_{\pm}(\lambda,u)$.

Finally, from (3.45) one introduces the trajectories in $\mathcal{D}_A$ generated through the evolution governed by (3.40), as done in (3.2) for (2.16), whose spacetime coordinates read

$$x(\lambda) = \frac{\zeta_+(\lambda,u_+) + \zeta_-(\lambda,u_-)}{2} \qquad\qquad t(\lambda) = \frac{\zeta_+(\lambda,u_+) - \zeta_-(\lambda,u_-)}{2} \tag{3.50}$$

where $\lambda \in \mathbb{R}$ and (u_+,u_-) are the light-cone coordinates of the point corresponding to $\lambda = 0$.

3.4 Heat

Any linear combinations of the above conserved currents defines a conserved current as well. From non-equilibrium thermodynamics [27], it is known that the heat density in the system is described by

$$\mathcal{M}(\tau;x,t) = \mathcal{E}(\tau;x,t) - \mu_c\, \varrho(\tau;x,t) - \mu_h\, \chi(\tau;x,t) \tag{3.51}$$

defined through (3.4), (3.19) and (3.24), where the electric charge and helicity chemical potentials are the combinations

$$\mu_e \equiv \mu_+ + \mu_- \qquad\qquad \mu_h \equiv \mu_+ - \mu_- \,. \tag{3.52}$$

Accordingly, the heat flow in the system is generated by the currents

$$q_x(\tau;x,t) = \mathcal{J}_x(\tau;x,t) - \mu_e\, j_x(\tau;x,t) - \mu_h\, k_x(\tau;x,t) \tag{3.53}$$

$$q_t(\tau;x,t) = \mathcal{J}_t(\tau;x,t) - \mu_e\, j_t(\tau;x,t) - \mu_h\, k_t(\tau;x,t)\,. \tag{3.54}$$

Combining (3.51) with (3.17), (3.23) and (3.32), for the total heat in the diamond $\mathcal{D}_A$ we have

$$\mathcal{M}_A = E_A - \mu_e\, Q_A - \mu_h\, \widetilde{Q}_A \tag{3.55}$$

which is independent of x, t and τ.

4 Infinite volume

In this section we consider the finite density representation of the CFT on the line, which is characterised by the mean values reported in section 4.1, and the modular Hamiltonian corresponding to the bipartition provided by an interval. The results of section 2.2 are employed to discuss the modular evolution of the fields (section 4.2), the modular conjugation and its geometric action (section 4.3). The modular correlators are considered in section 4.4.

JHEP08(2025)021

4.1 Finite density representation on the line

In the finite density representation of the CFT on the line, the mean values of the basic chiral fields described in section 2.1 are

$$\langle \phi_\pm(u) \rangle_{\mu_\pm} = 0 \qquad \langle j_\pm(u) \rangle_{\mu_\pm} = -\frac{\kappa \mu_\pm}{2\pi} \qquad \langle \mathcal{T}_\pm(u) \rangle_{\mu_\pm} = \frac{\kappa \mu_\pm^2}{4\pi} \,. \tag{4.1}$$

These expressions are obtained from the corresponding ones in the fundamental (ground state) representation π_0, where all these one-point function vanish (see the appendix A) through an automorphism $\gamma_\mu = \gamma_{\mu_+} \otimes \gamma_{\mu_-}$, as discussed in the appendix C. This automorphism provides the state $\Omega_{\mu_\pm}$ from the ground state Ω_0, which corresponds to $\mu_\pm = 0$. The finite density representation is given by $\pi_0 \circ \gamma_\mu$. In the following we denote $\pi_0 \circ \gamma_\mu[\mathcal{O}_\pm]$ just by $\mathcal{O}_\pm$, with a slight abuse of notation.

This procedure can be employed to find also the two-point functions of these fields in the finite density representation listed below, that are obtained from the ones in the fundamental representation, as explained in the appendix C). The two-point functions of $\phi_\pm$ are (see e.g. [28] for $\mu_\pm = 0$)

$$\langle \phi_\pm^*(u)\, \phi_\pm(v) \rangle_{\mu_\pm}^{\text{con}} = \frac{\mathrm{e}^{\mp \mathrm{i}\pi h_\pm}\, \mathrm{e}^{\pm \mathrm{i}\mu_\pm (u-v)}}{2\pi\, (u - v \mp \mathrm{i}\varepsilon)^{2h_\pm}} \qquad \langle \phi_\pm(u)\, \phi_\pm^*(v) \rangle_{\mu_\pm}^{\text{con}} = \frac{\mathrm{e}^{\mp \mathrm{i}\pi h_\pm}\, \mathrm{e}^{\mp \mathrm{i}\mu_\pm (u-v)}}{2\pi\, (u - v \mp \mathrm{i}\varepsilon)^{2h_\pm}} \,. \tag{4.2}$$

The two-point functions of $j_\pm$ contain the constant κ and read

$$\langle j_\pm(u)\, j_\pm(v) \rangle_{\mu_\pm}^{\text{con}} = \frac{\kappa}{4\pi^2} \frac{1}{(u - v \mp \mathrm{i}\varepsilon)^2} \tag{4.3}$$

while the two-point functions of $\mathcal{T}_\pm$ depend on the central charge c as follows

$$\langle \mathcal{T}_\pm(u)\, \mathcal{T}_\pm(v) \rangle_{\mu_\pm}^{\text{con}} = \frac{c}{8\pi^2} \frac{1}{(u - v \mp \mathrm{i}\varepsilon)^4} \,. \tag{4.4}$$

The positivity of (4.2)–(4.4) imply $h_\pm \geqslant 0$ (see the appendix D), $\kappa \geqslant 0$ and $c \geqslant 0$ respectively. Furthermore, we have that

$$\langle \mathcal{T}_\pm(u)\, j_\pm(v) \rangle_{\mu_\pm}^{\text{con}} = -\,\mu_\pm \, \langle j_\pm(u)\, j_\pm(v) \rangle_{\mu_\pm}^{\text{con}} \,. \tag{4.5}$$

The connected mixed correlators involving fields having different chiralities vanish identically.

When $t \pm x$ are chosen as light-cone coordinates, the $\mp \mathrm{i}\varepsilon$ must be replaced with $-\mathrm{i}\varepsilon$ in all the chiral two-point functions occurring in this manuscript.

4.2 Modular Hamiltonian

The results discussed in section 2.2 can be employed to investigate some modular Hamiltonians in two-dimensional CFT corresponding to the spatial bipartition provided by an interval [7–10].

In the following we consider a CFT on a line and in the finite density state characterised by the correlators reported in section 4.1. The spatial bipartition of the line is given by the interval $A = [a, b]$ and its complement $B = (-\infty, a) \cup (b, +\infty)$. In this setup, the modular Hamiltonian of the interval A reads [9, 11]

$$K_A = \int_A V(u_+) \left[\mathcal{T}_+(u_+) - \frac{\kappa \mu_+^2}{4\pi} \right] \mathrm{d}u_+ + \int_A V(u_-) \left[\mathcal{T}_-(u_-) - \frac{\kappa \mu_-^2}{4\pi} \right] \mathrm{d}u_- \tag{4.6}$$

JHEP08(2025)021

in terms of the chiral operators (2.7), with

$$V(u) = 2\pi \frac{(b-u)(u-a)}{b-a} = \frac{1}{w'(u)} \qquad\qquad u \in A \tag{4.7}$$

where

$$w(u) \equiv \frac{1}{2\pi} \log\left(-\frac{u-a}{u-b}\right). \tag{4.8}$$

The modular Hamiltonian (4.6) can be obtained by applying the automorphism γ_μ^{-1} described in the appendix C to the corresponding modular Hamiltonian in the fundamental representation (see (C.9)). Notice that the integrand in (4.6) corresponds to the special case of (3.24) where $V_\pm(u_\pm) = V(u_\pm)$ and $f_\pm(u_\pm) = -\frac{\kappa\mu_\pm^2}{4\pi} V(u_\pm)$.

The modular Hamiltonian of the complement B can be found by exchanging a and b in (4.7) and (4.8) (in the latter equation also the global sign in the argument of the logarithm must be inverted in order to have a well defined function); hence V changes its global sign. Notice that $-V(u) \geqslant 0$ when $u \in B$. This leads to

$$K_B = \int_B (-V(u_+)) \left[\mathcal{T}_+(u_+) - \frac{\kappa\mu_+^2}{4\pi}\right] \mathrm{d}u_+ + \int_B (-V(u_-)) \left[\mathcal{T}_-(u_-) - \frac{\kappa\mu_-^2}{4\pi}\right] \mathrm{d}u_- \,. \tag{4.9}$$

We remark that the weight functions in (4.6) and (4.9), which are given by $V(u)$ and $-V(u)$ respectively, are positive in the corresponding domains. The modular Hamiltonians (4.6) and (4.9) provide the full modular Hamiltonian for the bipartition and the finite density state $\Omega_{\mu_\pm}$ that we are considering, which reads

$$\begin{aligned} K &\equiv K_A \otimes \mathbf{1}_B - \mathbf{1}_A \otimes K_B \\ &= \int_{-\infty}^{\infty} V(u_+) \left[\mathcal{T}_+(u_+) - \frac{\kappa\mu_+^2}{4\pi}\right] \mathrm{d}u_+ + \int_{-\infty}^{\infty} V(u_-) \left[\mathcal{T}_-(u_-) - \frac{\kappa\mu_-^2}{4\pi}\right] \mathrm{d}u_- \,. \end{aligned} \tag{4.10}$$

We remark that, because of the choice $f_\pm(u_\pm) = -\frac{\kappa\mu_\pm^2}{4\pi} V(u_\pm)$, this full modular Hamiltonian satisfies $\langle K \rangle_\mu = 0$, which is a straightforward consequence of the constraint $K\,\Omega_{\mu_\pm} = 0$ (see eq. (V.2.7) of [1]). The full modular Hamiltonian (4.10) corresponds to the special case of (2.6) where $V_+(u) = V_-(u) = V(u)$ is the velocity (4.7) (which vanishes only at the endpoints of A) and $\mathcal{T}_\pm(u_\pm)$ are the operators in the finite density representation introduced in section 4.1.

The modular evolution generated by the full modular Hamiltonian (4.10) can be investigated by specialising the results discussed in section 2.2 to $V_+(u) = V_-(u) = V(u)$ given by (4.7). In this case (2.16) becomes

$$\xi_\pm(\tau, u) = \xi(\pm\tau, u) \qquad\qquad \xi(\tau, u) \equiv \frac{(b-u)\,a + (u-a)\,b\,\mathrm{e}^{2\pi\tau}}{(b-u) + (u-a)\,\mathrm{e}^{2\pi\tau}} \,. \tag{4.11}$$

Although this expression has been obtained for $u \in A$, it can extended to $u \in B$; indeed, it is invariant under the transformation that exchanges a and b and replaces τ with $-\tau$. Another way to find this result is to consider $\tilde{w}(u) = \frac{1}{2\pi} \log(\frac{u-b}{u-a})$ for $u \in B$ introduced above and observe that the expression $\tilde{w}^{-1}(\tilde{w}(u) - \tau)$ obtained from such $\tilde{w}(u)$ (see (2.16) combined with (4.10)) coincides with the one given in (4.11). Notice that $\xi(\tau, u)$ in (4.11)

JHEP08(2025)021

can be written in the form $\xi(\tau,u)=\frac{\alpha u+\beta}{\gamma u+\delta}$, with $\alpha=\frac{b\,\mathrm{e}^{2\pi\tau}-a}{b-a}$, $\beta=\frac{a\,b\,(1-\mathrm{e}^{2\pi\tau})}{b-a}$, $\gamma=\frac{\mathrm{e}^{2\pi\tau}-1}{b-a}$ and $\delta=\frac{b-a\,\mathrm{e}^{2\pi\tau}}{b-a}$; hence it is not a transformation of $\mathrm{SL}(2,\mathbb{R})$ for any value of τ because $\alpha\delta-\beta\gamma=\mathrm{e}^{2\pi\tau}$, which is different from one for $\tau\neq 0$.

For every $\tau\in\mathbb{R}$, we have that $\xi(\tau,u)\in A$ when $u\in A$ and $\xi(\tau,u)\in B$ when $u\in B$. Moreover, given $u\in\mathbb{R}$, one observes that $\xi(\tau,u)\to b$ as $\tau\to+\infty$ and $\xi(\tau,u)\to a$ as $\tau\to-\infty$. When $u\in B$, a finite value $\tau_\infty(u)$ for τ occurs such that $\xi(\tau,u)\to\pm\infty$ when $\tau\to\tau_\infty(u)^\pm$. It corresponds to the zero of the denominator of (4.11) and its explicit expression reads [29]

$$\tau_\infty(u)\equiv\frac{1}{2\pi}\,\log\!\left(\frac{u-b}{u-a}\right). \tag{4.12}$$

which is $\tau_\infty(u)<0$ when $u>b$ and $\tau_\infty(u)>0$ when $u<a$.

The modular evolutions of $\phi_\pm$, $j_\pm$ and $\mathcal{T}_\pm$ are obtained by plugging (4.11) into (2.18), (2.23) and (2.34) respectively. We remark that the Schwarzian derivative (2.35) for (4.11) vanishes identically, i.e. $\mathcal{S}_u[\xi](\tau,u)=0$.

From (3.2) and (4.11), we get the modular trajectories in the spacetime as follows

$$x(\tau)=\frac{\xi(\tau,u_+)+\xi(-\tau,u_-)}{2}\qquad\qquad t(\tau)=\frac{\xi(\tau,u_+)-\xi(-\tau,u_-)}{2} \tag{4.13}$$

where (u_+,u_-) are the light-cone coordinates of the spacetime point corresponding to $\tau=0$.

The domain of dependence $\mathcal{D}_A$ of the interval A is the diamond made by the points with light-cone coordinates $u_\pm\in A$ and it corresponds to the grey rhombus in figure 1. Its vertices P_a, P_b, $P_{+\infty}$ and $P_{-\infty}$ have light-cone coordinates $(u_+,u_-)\in\{(a,a),(b,b),(b,a),(a,b)\}$ respectively. Let us introduce the partition of $\mathcal{D}_A$ provided by the light rays from its center P_c, whose light-cone coordinates are $u_+=u_-=\frac{a+b}{2}$ (see the dot-dashed segments in $\mathcal{D}_A$ in figure 1). This gives $\mathcal{D}_A=\mathcal{D}_{\mathrm{R}}\cup\mathcal{D}_{\mathrm{L}}\cup\mathcal{D}_{\mathrm{F}}\cup\mathcal{D}_{\mathrm{P}}$, where $\mathcal{D}_i$ belongs to the right wedge, the left wedge, the future cone and the past cone of P_c for $i\in\{\mathrm{R},\mathrm{L},\mathrm{F},\mathrm{P}\}$ respectively. A modular trajectory (4.13) whose initial point corresponding to $\tau=0$ belongs to $\mathcal{D}_A$ entirely stays within $\mathcal{D}_A$, for any real value of τ. In particular, its endpoints are the vertices $P_{+\infty}$ and $P_{-\infty}$, which are reached as $\tau\to+\infty$ and $\tau\to-\infty$ respectively. In figure 1 the red and blue solid lines are the modular trajectories whose initial points are the red and blue dots respectively. The modular trajectories whose initial point has light-cone coordinates (u_+,u_-) such that $u_\pm\in A$ span the diamond $\mathcal{D}_A$.

As for region $\mathcal{R}_A$ made by the points with light-cone coordinates $u_\pm\in B$ (light blue region in figure 1), it can be naturally partitioned into four regions, i.e. $\mathcal{R}_A=\mathcal{R}_{\mathrm{R}}\cup\mathcal{R}_{\mathrm{L}}\cup\mathcal{R}_{\mathrm{F}}\cup\mathcal{R}_{\mathrm{P}}$, where $\mathcal{R}_i$ is the infinite region that shares a vertex of $\mathcal{D}_A$ with $\mathcal{D}_i$ and belongs to the right wedge, the left wedge, the future cone and the past cone of P_c for $i\in\{\mathrm{R},\mathrm{L},\mathrm{F},\mathrm{P}\}$ respectively. The modular trajectories (4.13) with initial points at $\tau=0$ in $\mathcal{R}_A$ span the entire domain $\mathcal{R}_A$ (in figure 1, see e.g. the green, yellow and brown solid lines, whose initial points are the dots having the corresponding color). A modular trajectories which does not belong to the vertical line passing through $P_{+\infty}$ and $P_{-\infty}$ has a non trivial intersection with $\mathcal{R}_{\mathrm{P}}$, $\mathcal{R}_{\mathrm{F}}$ and either $\mathcal{R}_{\mathrm{R}}$ or $\mathcal{R}_{\mathrm{L}}$, depending on whether the x-coordinate of its initial point at $\tau=0$ (whose light-cone coordinate are $u_\pm$) is either $x>(a+b)/2$ or $x<(a+b)/2$ respectively (instead, the single modular trajectory belonging to the vertical line passing through $P_{+\infty}$ and $P_{-\infty}$ intersects $\mathcal{R}_{\mathrm{P}}$ and $\mathcal{R}_{\mathrm{F}}$ only). The two transitions from $\mathcal{R}_{\mathrm{P}}$ to $\mathcal{R}_i$ and from $\mathcal{R}_i$

JHEP08(2025)021

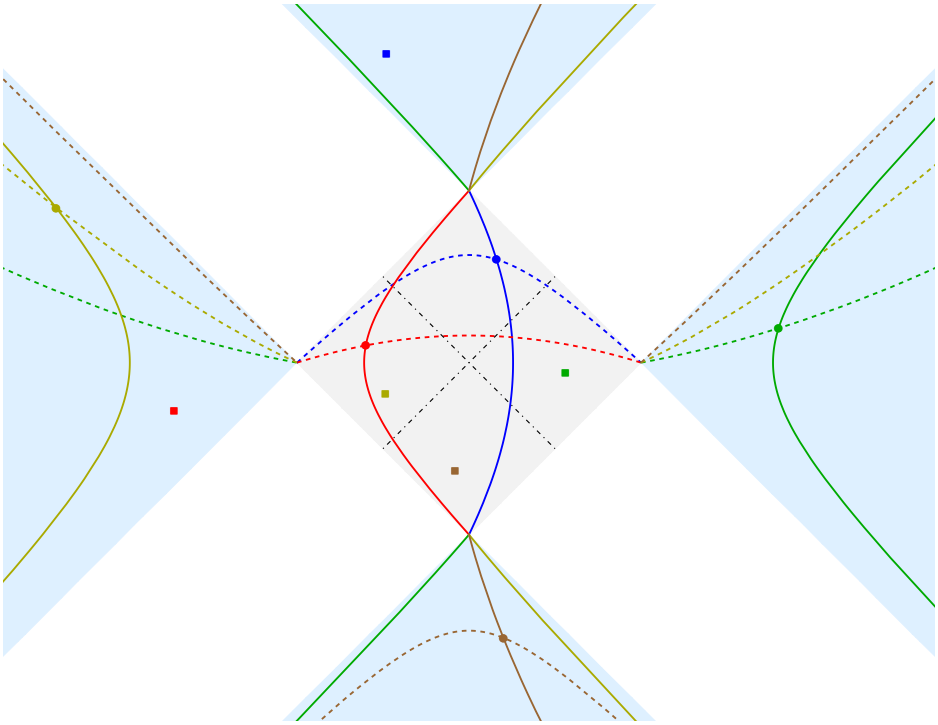

Figure 1. Modular trajectories generated by either the modular Hamiltonian (4.10) (solid lines) or the modular momentum (4.14) (dashed lines), obtained from (4.13) and (4.15) respectively. The coloured squares denote the images through the modular conjugation (4.22) of the spacetime points corresponding to the dots having the same colour. The dot dashed segments identify the partition $\mathcal{D}_A = \mathcal{D}_{\rm R} \cup \mathcal{D}_{\rm L} \cup \mathcal{D}_{\rm F} \cup \mathcal{D}_{\rm P}$ of the diamond $\mathcal{D}_A$.

to $\mathcal{R}_{\rm F}$, where $i \in \{{\rm L}, {\rm R}\}$, occur at two finite values of τ given by $\tau_\infty(u_+)$ and $\tau_\infty(u_-)$, in terms of $\tau_\infty(u)$ introduced in (4.12) [29].

We remark that all the modular trajectories arrive to $P_{+\infty}$ and $P_{-\infty}$ as $\tau \to +\infty$ and $\tau \to -\infty$ respectively, independently of whether the initial point is either in $\mathcal{D}_A$ or in $\mathcal{R}_A$.

The modular momentum operator is obtained by specialising (3.40) to the case that we are investigating, finding

$$P \equiv \int_{-\infty}^{\infty} V(u_+) \left[\mathcal{T}_+(u_+) - \frac{\kappa \mu_+^2}{4\pi} \right] {\rm d}u_+ - \int_{-\infty}^{\infty} V(u_-) \left[\mathcal{T}_-(u_-) - \frac{\kappa \mu_-^2}{4\pi} \right] {\rm d}u_- \tag{4.14}$$

where $V(u)$ has been introduced in (4.7). This operator provides a transformation of the fields that can be written by specialising the results of section 3.3 to $V_+(u) = V_-(u) = V(u)$. The corresponding modular trajectories in the spacetime are obtained from (3.50) in the same way and the result reads

$$x(\lambda) = \frac{\zeta(\lambda, u_+) + \zeta(\lambda, u_-)}{2} \qquad t(\lambda) = \frac{\zeta(\lambda, u_+) - \zeta(\lambda, u_-)}{2} \tag{4.15}$$

where $\lambda \in \mathbb{R}$ and (u_+, u_-) are the light-cone coordinates of the initial point at $\lambda = 0$. The initial point can be either in $\mathcal{D}_A$ or in $\mathcal{R}_A$ and the entire modular trajectory (4.15) belongs to the same region for all finite real values of λ, reaching P_a and P_b as $\lambda \to -\infty$ and $\lambda \to +\infty$

JHEP08(2025)021

respectively. In figure 1 the dashed curves we show some modular trajectories generated by the momentum operator, whose initial points are the dots with the same colour.

The above discussion is based on the fact that $V_+(u) = V_-(u)$, given by (4.7). Since the assumption $V_+ = V_-$ has not been employed throughout section 2, it is straightforward to extend our analysis to the boosted interval, which is characterised by two different bipartitions along the chiral directions, determined by the interval (a_+, b_+) and (a_-, b_-) for u_+ and u_- directions respectively. When the CFT_2 is at finite densities, the modular Hamiltonian to consider is (2.6) with the following weight functions

$$V_\pm(u) \equiv 2\pi \frac{(b_\pm - u)(u - a_\pm)}{b_\pm - a_\pm} = \frac{1}{w'_\pm(u)} \qquad u \in (a_\pm, b_\pm) \tag{4.16}$$

where

$$w_\pm(u) \equiv \frac{1}{2\pi} \log\left(-\frac{u - a_\pm}{u - b_\pm}\right). \tag{4.17}$$

From section 2.2, we have that the modular evolution of a primary chiral field is given by (2.18), where $\xi_\pm(\tau, u)$ is obtained by specifying (2.16) to this case. This leads to

$$\xi_\pm(\tau, u) = \frac{(b_\pm - u)\, a_\pm + (u - a_\pm)\, b_\pm\, \mathrm{e}^{\pm 2\pi\tau}}{(b_\pm - u) + (u - a_\pm)\, \mathrm{e}^{\pm 2\pi\tau}} \tag{4.18}$$

which reduce to (4.11) when $a_+ = a_-$ and $b_+ = b_-$, as expected. As for the modular evolution generated by the modular generalised momentum (3.40) defined through the weight functions (4.16) characterising the boosted interval, for a primary chiral field we find (3.48) with

$$\zeta_\pm(\lambda, u) = \frac{(b_\pm - u)\, a_\pm + (u - a_\pm)\, b_\pm\, \mathrm{e}^{2\pi\lambda}}{(b_\pm - u) + (u - a_\pm)\, \mathrm{e}^{2\pi\lambda}}\,. \tag{4.19}$$

From (4.18) and (4.19) it is straightforward to obtain the generalisation of figure 1 corresponding to a region of spacetime determined by two different intervals (a_+, b_+) and (a_-, b_-) along the chiral directions parameterised by u_+ and u_- respectively.

Let us conclude this discussion with a brief comment on the relation between the operator (4.10) and the Tomita-Takesaki modular theory. Referring for details to [30], here we observe that the K-flow generated by the operator (4.10) is well defined for conformal fields with any dimension $h_\pm \geqslant 0$. With some abuse of terminology, such flow is usually called modular flow, although strictly speaking it can be associated with the Tomita-Takesaki theory only for quantum fields which are local, i.e. that either commute or anticommute at spacelike distances. In CFT, this is certainly the case for fields with dimensions $h_\pm \in \mathbb{Z}$ and $h_\pm \in \mathbb{Z} + \frac{1}{2}$. Hence, according to section 2, the modular theory applies for the currents describing the transport of electric charge and helicity ($h_\pm = 1$) and of energy ($h_\pm = 2$). With the exception of appendix B, in the following we focus on the modular properties of these currents.

4.3 Modular conjugation

The modular theory of Tomita and Takesaki [1, 31–34] is constructed through the modular operator e^{-K}, written in terms of the full modular Hamiltonian, and the modular conjugation J, an antiunitary operator which leaves the state invariant and satisfies $J = J^* = J^{-1}$. For

JHEP08(2025)021

the bipartition and the state of the CFT we are considering, the modular conjugation has a geometric action implemented by the real function $\mathrm{j} : \mathbb{R} \to \mathbb{R}$ which can be obtained by setting $\tau = \pm \mathrm{i}/2$ in (4.11) and reads [1]

$$\mathrm{j}(u) \equiv \frac{a+b}{2} + \frac{\left(\frac{b-a}{2}\right)^2}{u - \frac{a+b}{2}} \tag{4.20}$$

which is a bijective and idempotent function sending A onto B. The map (4.20) is invariant under $a \leftrightarrow b$ and satisfies $\mathrm{j}'(u) < 0$. We remark that (4.11) and (4.20) commute, namely

$$\mathrm{j}(\xi(\tau, u)) = \xi(\tau, \mathrm{j}(u)) \,. \tag{4.21}$$

Notice that $\mathrm{j}(u)$ in (4.20) becomes $\mathrm{j}(u) = 2a - u$ as $b \to +\infty$ and $\mathrm{j}(u) = 2b - u$ as $a \to -\infty$.

In Minkowski spacetime, the geometric action of the modular conjugation J associated to the state and the bipartition we are investigating can be written through (4.20) as follows

$$\tilde{x}(x,t) \equiv \frac{\mathrm{j}(u_+) + \mathrm{j}(u_-)}{2} \qquad \tilde{t}(x,t) \equiv \frac{\mathrm{j}(u_+) - \mathrm{j}(u_-)}{2} \,. \tag{4.22}$$

In figure 1 the points labelled by coloured squares are the images through (4.22) of the points labelled by dots having the same colour. Considering the partitions of $\mathcal{D}_A$ and $\mathcal{R}_A$ introduced in section 4.2, we have that, for any assigned $i \in \{\mathrm{R}, \mathrm{L}, \mathrm{F}, \mathrm{P}\}$, the idempotent map (4.22) sends $\mathcal{D}_i$ onto $\mathcal{R}_i$ in a bijective way.

The image of the modular trajectories (4.13) through (4.22) has been studied e.g. in [29]. Within the context of the gauge/gravity correspondence, the holographic dual of (4.22) tor $t = 0$ has been discussed [29, 35] by employing the geodesic bit threads [36, 37].

Considering a modular trajectory (4.13) in $\mathcal{D}_A$ with initial point $P \in \mathcal{D}_A$ having light-cone coordinates (u_+, u_-), its image under (4.22) belongs to $\mathcal{R}_A$ and the spacetime coordinates of its generic point read [29]

$$\tilde{x}(\tau) = \frac{\mathrm{j}(\xi(\tau, u_+)) + \mathrm{j}(\xi(-\tau, u_-))}{2} \qquad \tilde{t}(\tau) = \frac{\mathrm{j}(\xi(\tau, u_+)) - \mathrm{j}(\xi(-\tau, u_-))}{2} \tag{4.23}$$

which can be written in an equivalent form by employing (4.21).

In [29, 30] it has been observed that the union of the modular trajectory (4.13) in $\mathcal{D}_A$ and of the corresponding curve in $\mathcal{R}_A$ obtained through (4.23) provides the hyperbola $\mathcal{I}_P$ defined as follows

$$\big[x(\tau) - x_0\big]^2 - t(\tau)^2 = \kappa^2 \qquad \big[\tilde{x}(\tau) - x_0\big]^2 - \tilde{t}(\tau)^2 = \kappa_0^2 \tag{4.24}$$

whose parameters are

$$x_0 \equiv \frac{u_+ \, u_- - a \, b}{u_+ + u_- - (a+b)} \qquad \kappa_0 \equiv \frac{\sqrt{(b-u_+)(u_+ - a)\,(b-u_-)(u_- - a)}}{u_+ + u_- - (a+b)} \tag{4.25}$$

in terms of the light-cone coordinates of the initial point P.

JHEP08(2025)021

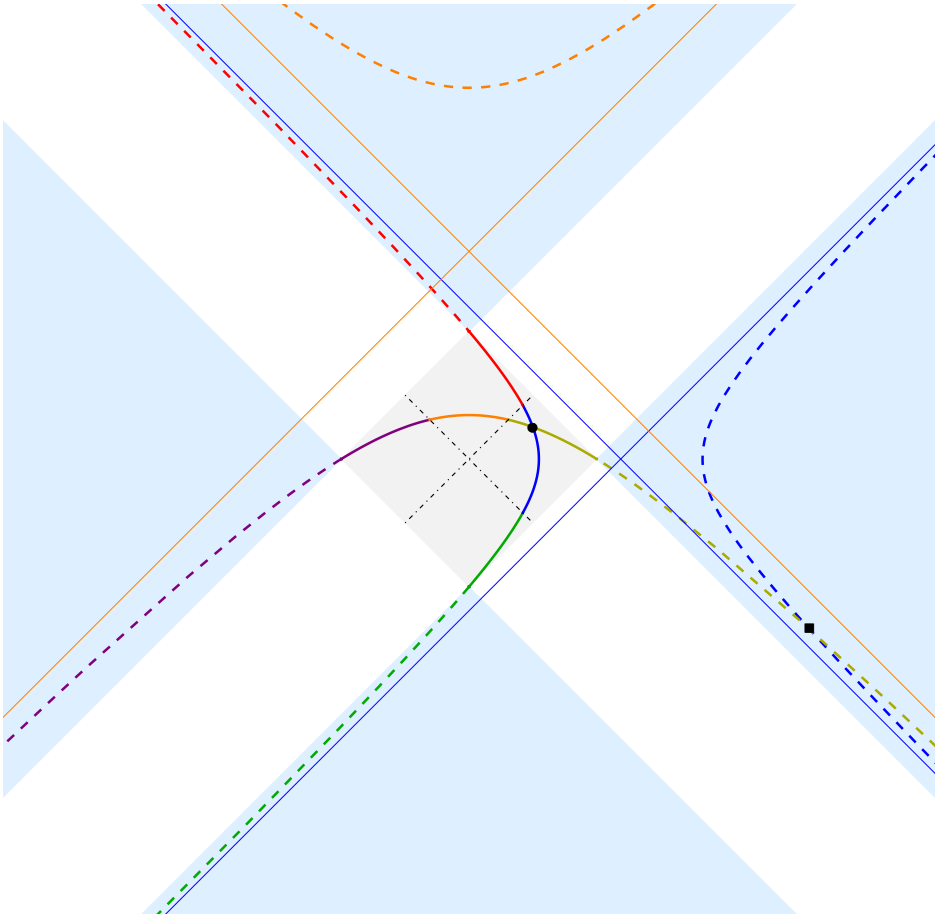

Figure 2. The modular hyperbolae $\mathcal{I}_P$ in (4.24) correspond to the red, blue and green arcs, while the modular hyperbolae $\widetilde{\mathcal{I}}_P$ in (4.27) is made by the purple, orange and dark yellow arcs. The asymptotes of $\mathcal{I}_P$ and $\widetilde{\mathcal{I}}_P$ are the orange and blue thin straight lines respectively.

In figure 2, the point P corresponds to the black dot and its modular trajectory has been partitioned into the green, blue and red solid arcs, corresponding to the intersection of the modular trajectory with different $\mathcal{D}_i$, with $i \in \{\mathrm{R}, \mathrm{L}, \mathrm{F}, \mathrm{P}\}$. The black square is the image of P under (4.22) and the image of each arc through (4.22) is indicated by the dashed curve with the same colour. The asymptotes of the hyperbolae (4.24) are $t = x - x_0$ and $t = -x + x_0$ (see the blue solid thin straight lines in figure 2).

It is worth considering also the modular trajectory (4.15) provided by the evolution generated by the modular momentum operator (4.14) having the same point $P \in \mathcal{D}_A$ employed above as initial point at $\lambda = 0$, where $\lambda \in \mathbb{R}$ is the modular parameter. In figure 2, this modular trajectory has been partitioned into the purple, orange and dark yellow solid arcs, which correspond to the intersection of the modular trajectory with different $\mathcal{D}_i$, with $i \in \{\mathrm{R}, \mathrm{L}, \mathrm{F}, \mathrm{P}\}$. The image of the modular trajectory (4.15) through (4.22) belongs to $\mathcal{R}_A$ and reads

$$\tilde{x}(\lambda) = \frac{\mathrm{j}(\zeta(\lambda, u_+)) + \mathrm{j}(\zeta(\lambda, u_-))}{2} \qquad \tilde{t}(\lambda) = \frac{\mathrm{j}(\zeta(\lambda, u_+)) - \mathrm{j}(\zeta(\lambda, u_-))}{2} \tag{4.26}$$

JHEP08(2025)021

In figure 2, the images under the inversion (4.22) of the solid arcs in purple, orange and dark yellow partitioning the modular trajectory obtained from (4.15) are the dashed arcs having the corresponding colour.

By adapting the construction of the hyperbola $\mathcal{I}_P$ to the evolution generated by the modular momentum operator (4.14), here we observe that the union of the modular trajectory (4.15) and of its image under the map (4.22) described by (4.26) provide the hyperbola $\widetilde{\mathcal{I}}_P$ given by

$$\big[\,t(\lambda)-t_0\,\big]^2-\left[\,x(\lambda)-\frac{a+b}{2}\,\right]^2=\lambda^2 \qquad\qquad \big[\,\tilde{t}(\lambda)-t_0\,\big]^2-\left[\,\tilde{x}(\lambda)-\frac{a+b}{2}\,\right]^2=\tilde{\kappa}_0^2 \tag{4.27}$$

where the parameters are

$$t_0 \equiv \frac{(u_+ - \frac{a+b}{2})(u_- - \frac{a+b}{2}) - (\frac{b-a}{2})^2}{u_- - u_+} \qquad\qquad \tilde{\kappa}_0 \equiv \frac{\sqrt{(b-u_+)(u_+-a)\,(b-u_-)(u_--a)}}{u_+-u_-} \tag{4.28}$$

in terms of the light-cone coordinates of the initial point P. These expressions are well defined whenever $u_+ \neq u_-$; indeed, for $u_+ = u_-$ the hyperbola $\widetilde{\mathcal{I}}_P$ becomes the horizontal line $t=0$. The two hyperbolas $\mathcal{I}_P$ and $\widetilde{\mathcal{I}}_P$ intersect at $P \in \mathcal{D}_A$ and at its image under (4.22) in $\mathcal{R}_A$.

It is worth describing the action of the modular conjugation on the fields of the CFT considered in section 2. In the literature, this transformation has been considered e.g. in [38, 39]. Since the geometric action of the modular conjugation is obtained from (4.11) at $\tau = \pm\,\mathrm{i}/2$, the action of J on the basic fields of the CFT can be found by combining the fact that J is antiunitary with (2.18), (2.20), (2.23) and (2.34). Thus, for the primaries we have

$$J\,\phi_\pm(u)\,J = \mathrm{e}^{\mp \mathrm{i}\mu_\pm(\mathrm{j}(u)-u)}\,\mathrm{j}'(u)^{h_\pm}\,\phi_\pm^*(\mathrm{j}(u)) \tag{4.29}$$

$$J\,\phi_\pm^*(u)\,J = \mathrm{e}^{\pm \mathrm{i}\mu_\pm(\mathrm{j}(u)-u)}\,\mathrm{j}'(u)^{h_\pm}\,\phi_\pm(\mathrm{j}(u)) \tag{4.30}$$

where, from (4.20), we have that $\mathrm{j}'(u) < 0$. We remark that $\mathrm{j}'(u) \to -1$ as either $b \to +\infty$ or $a \to -\infty$. As for the currents and the operators (2.7) containing the energy-momentum tensor, which are hermitean operators, we find respectively

$$J\,j_\pm(u)\,J = \mathrm{j}'(u)\,j_\pm(\mathrm{j}(u)) - \frac{\kappa\mu_\pm}{2\pi}\,\big[\,1-\mathrm{j}'(u)\,\big] \tag{4.31}$$

and

$$J\,\mathcal{T}_\pm(u)\,J = \mathrm{j}'(u)^2\,\mathcal{T}_\pm(\mathrm{j}(u)) + \frac{\kappa\mu_\pm^2}{4\pi}\,\Big[\,1-\mathrm{j}'(u)^2\,\Big] \tag{4.32}$$

where in the last expression we used that the Schwarzian derivative (see (2.35)) of (4.20) vanishes identically, i.e. $\mathcal{S}_u[\mathrm{j}](u) = 0$.

The transformation rule (4.32) can be employed to observe that

$$\begin{aligned} J\left(\int_a^b V(u)\,\mathcal{T}_\pm(u)\,\mathrm{d}u\right)J &= \int_a^b \mathrm{j}'(u)\,V(u)\,\mathcal{T}_\pm(\mathrm{j}(u))\,\mathrm{j}'(u)\,\mathrm{d}u + \text{const} \\ &= -\left[\int_{-\infty}^a V(u)\,\mathcal{T}_\pm(u)\,\mathrm{d}u + \int_b^{+\infty} V(u)\,\mathcal{T}_\pm(u)\,\mathrm{d}u\right] + \text{const} \end{aligned} \tag{4.33}$$

where we used that (4.7) and (4.20) satisfy the following identity

$$\mathrm{j}'(u)\,V(u) = V(\mathrm{j}(u))\,. \tag{4.34}$$

JHEP08(2025)021

By applying (4.33) to (4.6), it is straightforward to find that (4.9) can be written as $K_B = J\,K_A\,J$; hence the full modular Hamiltonian (4.10) can be equivalently expressed in the following suggestive form

$$K \equiv K_A \otimes \mathbf{1}_B - \mathbf{1}_A \otimes (J\,K_A\,J) \tag{4.35}$$

Since $J\,\Omega_{\mu_\pm} = \Omega_{\mu_\pm}$, taking the mean values of (4.29), (4.30), (4.31) and (4.32) in the l.h.s.'s one finds $\langle\phi_\pm(u)\rangle_{\mu_\pm}$, $\langle\phi^*_\pm(u)\rangle_{\mu_\pm}$, $\langle j_\pm(u)\rangle_{\mu_\pm}$ and $\langle\mathcal{T}_\pm(u)\rangle_{\mu_\pm}$ respectively. By using (4.1) in the corresponding r.h.s.'s, consistency is observed; indeed, the r.h.s.'s of the expressions in (4.1) are obtained.

The modular conjugation J allows us to investigate the modular evolution in $\mathcal{R}_A$. Indeed, considering a chiral operator $\mathcal{O}_\pm(u)$ placed at $u \in B$, i.e. in the domain complementary to A on the line, its modular evolution $\mathcal{O}_\pm(\tau, u)$ can be written as

$$\mathcal{O}_\pm(\tau,u) = \mathrm{e}^{\mathrm{i}K\tau}\,\mathcal{O}_\pm(u)\,\mathrm{e}^{-\mathrm{i}K\tau} = JJ\,\mathrm{e}^{\mathrm{i}K\tau}\,\mathcal{O}_\pm(u)\,\mathrm{e}^{-\mathrm{i}K\tau}JJ = J\left[\mathrm{e}^{\mathrm{i}K\tau}(J\,\mathcal{O}_\pm(u)\,J)\,\mathrm{e}^{-\mathrm{i}K\tau}\right]J \tag{4.36}$$

where we used that J is idempotent and that $J\,\mathrm{e}^{\mathrm{i}K\tau}J = \mathrm{e}^{\mathrm{i}K\tau}$ (see e.g. eq. (V.2.9) of [1]). In the last expression of (4.36), the operator $J\,\mathcal{O}_\pm(u)\,J$ is located in A; hence the same holds for its modular evolution, which corresponds to the operator within the square brackets in the last expression of (4.36). In the appendix E we have obtained explicit expressions for (4.36) when $\mathcal{O}_\pm$ is either $\phi_\pm$ or $j_\pm$ or $\mathcal{T}_\pm$, finding that the expressions for the modular evolutions given by (2.18), (2.20), (2.23) and (2.34) with $\xi_\pm(\tau, u)$ reported in (4.11) hold also when $u \in B$.

4.4 Modular correlators

The two-point functions of the primaries, of the currents and of the energy-momentum tensor along the modular evolution generated by the full modular Hamiltonian (4.10) can be written by combining the results discussed in section 2.2 with the expressions reported in section 4.1.

As for the one-point functions, from (4.1) we can take the mean values of (2.18), (2.20), (2.23) and (2.34) with $\xi_\pm(\tau, u)$ given by (4.11), finding that they are independent of τ, i.e. $\langle\phi_\pm(u)\rangle_{\mu_\pm} = \langle\phi_\pm(\tau,u)\rangle_{\mu_\pm}$ for the primaries, $\langle j_\pm(u)\rangle_{\mu_\pm} = \langle j_\pm(\tau,u)\rangle_{\mu_\pm}$ for the currents and $\langle\mathcal{T}_\pm(u)\rangle_{\mu_\pm} = \langle\mathcal{T}_\pm(\tau,u)\rangle_{\mu_\pm}$ for the operators (2.7).

In order to investigate the modular two-point functions, we first observe that, when $u \neq v$ and $\tau_1 \neq \tau_2$ are real, for (4.11) we have

$$\frac{\partial_u\xi(\tau_1,u)\,\partial_v\xi(\tau_2,v)}{\big[\xi(\tau_1,u)-\xi(\tau_2,v)\big]^2} = \left(\frac{R(\tau_{12};u,v)}{u-v}\right)^2 \tag{4.37}$$

where we have introduced

$$R(\tau;u,v) \equiv \frac{\mathrm{e}^{2\pi w(u)} - \mathrm{e}^{2\pi w(v)}}{\mathrm{e}^{2\pi w(u)+\pi\tau} - \mathrm{e}^{2\pi w(v)-\pi\tau}} = \frac{(u-a)(v-b)-(u-b)(v-a)}{(u-a)(v-b)\,\mathrm{e}^{\pi\tau} - (u-b)(v-a)\,\mathrm{e}^{-\pi\tau}} \tag{4.38}$$

which satisfies

$$R(\tau=0;u,v) = 1 \qquad R(-\tau;v,u) = R(\tau;u,v) \qquad R(\tau+\mathrm{i}\,;u,v) = -R(-\tau;v,u) \tag{4.39}$$

JHEP08(2025)021

In the derivation of (4.37) we used that

$$\xi(\tau_1,u)-\xi(\tau_2,v)=\frac{p(\tau_1,u)\,p(\tau_2,v)}{R(\tau_{12};u,v)}\,(u-v) \tag{4.40}$$

in terms of (4.38) and of

$$p(\tau,u)\equiv\frac{(b-a)\,\mathrm{e}^{\pi\tau}}{b-u+(u-a)\,\mathrm{e}^{2\pi\tau}}\qquad\qquad q(\tau,u)\equiv b-u+(u-a)\,\mathrm{e}^{2\pi\tau}\,. \tag{4.41}$$

The dependence on τ_{12} in (4.37), which is not evident in the l.h.s., occurs because the product $q(\tau_1,u)\,q(\tau_2,v)$ simplifies in the ratio (see (4.40)). Notice that $\mathrm{e}^{2\pi w(u)}$ in (4.37) is well defined for $u\in\mathbb{R}$, although $w(u)$ in (4.8) holds for $u\in A$. Moreover, we remark that (4.37) is invariant under the simultaneous exchange $a\leftrightarrow b$ and $\tau_1\leftrightarrow\tau_2$.

For the primaries $\phi_\pm$, from (2.18), (2.20), (4.1), (4.2) and (4.37), one finds the following modular correlators

$$\begin{aligned}\langle\phi^*_\pm(\tau_1,u)\,\phi_\pm(\tau_2,v)\rangle^{\mathrm{con}}_{\mu_\pm}&=\\&=\mathrm{e}^{\mp\mathrm{i}\mu_\pm[\xi_\pm(\tau_1,u)-\xi_\pm(\tau_2,v)-u+v]}\big[\partial_u\xi_\pm(\tau_1,u)\,\partial_v\xi_\pm(\tau_2,v)\big]^{h_\pm}\langle\phi^*_\pm\big(\xi_\pm(\tau_1,u)\big)\,\phi_\pm\big(\xi_\pm(\tau_2,v)\big)\rangle_{\mu_\pm}\\&=\frac{\mathrm{e}^{\pm\mathrm{i}\mu_\pm(u-v)}}{2\pi\,\mathrm{e}^{\pm\mathrm{i}\pi h_\pm}}\,W_\pm(\pm\tau_{12};u,v)^{2h_\pm}\end{aligned} \tag{4.42}$$

and

$$\langle\phi_\pm(\tau_1,u)\,\phi^*_\pm(\tau_2,v)\rangle^{\mathrm{con}}_{\mu_\pm}=\frac{\mathrm{e}^{\mp\mathrm{i}\mu_\pm(u-v)}}{2\pi\,\mathrm{e}^{\pm\mathrm{i}\pi h_\pm}}\,W_\pm(\pm\tau_{12};u,v)^{2h_\pm} \tag{4.43}$$

where we have introduced

$$W_\pm(\tau;u,v)\equiv\frac{\mathrm{e}^{2\pi w(u)}-\mathrm{e}^{2\pi w(v)}}{u-v}\,\frac{1}{\mathrm{e}^{2\pi w(u)+\pi\tau}-\mathrm{e}^{2\pi w(v)-\pi\tau}\mp\mathrm{i}\varepsilon}\,. \tag{4.44}$$

When either $u\neq v$ or $\tau\neq 0$, we can set $\varepsilon=0$ and $W_\pm(\tau;u,v)$ becomes

$$W(\tau;u,v)\equiv\frac{R(\tau;u,v)}{u-v} \tag{4.45}$$

in terms of (4.38). Notice that the Hilbert space structure implies that (4.42) satisfies

$$\langle\phi^*_\pm(\tau_1,u)\,\phi_\pm(\tau_2,v)\rangle^{\mathrm{con}}_{\mu_\pm}=\overline{\langle\phi^*_\pm(\tau_2,v)\,\phi_\pm(\tau_1,u)\rangle^{\mathrm{con}}_{\mu_\pm}} \tag{4.46}$$

where the overline denotes the complex conjugation.

As for the currents $j_\pm$, from (2.23), (4.1), (4.3) and (4.37), their modular correlators read

$$\begin{aligned}\langle j_\pm(\tau_1,u)\,j_\pm(\tau_2,v)\rangle^{\mathrm{con}}_{\mu_\pm}&=\big[\partial_u\xi_\pm(\tau_1,u)\,\partial_v\xi_\pm(\tau_2,v)\big]\,\langle j_\pm\big(\xi_\pm(\tau_1,u)\big)\,j_\pm\big(\xi_\pm(\tau_2,v)\big)\rangle_{\mu_\pm}\\&=\frac{\kappa}{4\pi^2}\,W_\pm(\pm\tau_{12};u,v)^2\,.\end{aligned} \tag{4.47}$$

Similarly, for the modular correlators of the operators (2.7), which contains the energy-momentum tensor, from (2.34), (4.1), (4.4) and (4.37), we find

$$\begin{aligned}\langle\mathcal{T}_\pm(\tau_1,u)\,\mathcal{T}_\pm(\tau_2,v)\rangle^{\mathrm{con}}_{\mu_\pm}&=\big[\partial_u\xi_\pm(\tau_1,u)\,\partial_v\xi_\pm(\tau_2,v)\big]^2\,\langle\mathcal{T}_\pm\big(\xi_\pm(\tau_1,u)\big)\,\mathcal{T}_\pm\big(\xi_\pm(\tau_2,v)\big)\rangle_{\mu_\pm}\\&=\frac{c}{8\pi^2}\,W_\pm(\pm\tau_{12};u,v)^4\,.\end{aligned} \tag{4.48}$$

We remark that these modular correlators are functions of τ_{12} which depend on t_1 and t_2 separately; hence the modular energy is conserved along the modular evolution (see section 3.2), while the conventional energy is not. Furthermore, according to the discussion reported at the end of section 4.3 and in the appendix E, we have that the expressions (4.42), (4.43), (4.47) and (4.48) for the modular correlators hold for any $u, v \in \mathbb{R}$.

Since for (4.44) the following property holds

$$W_{\pm}(\tau + \mathrm{i}; u, v) = W_{\pm}(\tau - \mathrm{i}; u, v) = W_{\pm}(-\tau; v, u) \tag{4.49}$$

the modular correlators (4.42), (4.43), (4.47) and (4.48) satisfy the KMS condition with modular inverse temperature $\tilde{\beta} = 1$. This is a characterising feature of the modular correlators that exposes the thermal nature of the modular evolution. Furthermore, the validity of this condition confirms the expression (4.6) for the modular Hamiltonian (this criterion has been adopted e.g. in [40] to confirm the expression of the modular Hamiltonian of disjoint intervals on the line for the massless Dirac field in the ground state, found in [41]).

In the appendix D we also provide a consistency check for (4.42) based on the modular reflection positivity property (see e.g. [38]).

Let us highlight that, when $\tau \neq 0$, the limit $v \to u$ of (4.44) is well defined and reads

$$\lim_{v \to u} W_{\pm}(\tau; u, v) = \frac{\pi}{V(u)\, \sinh(\pi\tau \mp \mathrm{i}\varepsilon)} \,. \tag{4.50}$$

This observation will be employed in section 5.3 in a crucial way.

From the properties of the modular conjugation, for a chiral operator $\mathcal{O}_{\pm}$ we have

$$\langle \mathcal{O}^*_{\pm}(\tau_1, u)\, \mathcal{O}_{\pm}(\tau_2, v) \rangle^{\mathrm{con}}_{\mu_{\pm}} = \langle \big[J\, \mathcal{O}^*_{\pm}(\tau_2, v)\, J \big] \big[J\, \mathcal{O}_{\pm}(\tau_1, u)\, J \big] \rangle^{\mathrm{con}}_{\mu_{\pm}} \tag{4.51}$$

By employing the following identity

$$W_{\pm}(\tau, u, v)^2 = \mathrm{j}'(u)\, \mathrm{j}'(v)\, W_{\pm}(-\tau, \mathrm{j}(v), \mathrm{j}(u))^2 \tag{4.52}$$

we checked that the r.h.s.'s of (4.29), (4.30) (4.31) and (4.32) are consistent with (4.51).

The analyses discussed above can be extended to investigate the correlators of the fields whose evolution is determined by the momentum operator (see (4.14)–(4.15) and section 3.3). It is straightforward to adapt the expressions (4.42), (4.43), (4.47) and (4.48) to these flows, finding correlators that satisfy the corresponding KMS condition, whose validity is based on the property (4.49) for (4.44).

5 Modular transport and fluctuations

In this section we consider the modular evolution $\mathcal{O}(\tau; x, t) \equiv \mathrm{e}^{\mathrm{i}\tau K} \mathcal{O}(x, t)\, \mathrm{e}^{-\mathrm{i}\tau K}$ of some observables $\mathcal{O}$ (essentially currents and densities) of the CFT in the finite density representation and for the bipartition given by an interval on the line. In unitary quantum field theory, the sequence of connected correlation functions $\{\langle \mathcal{O}(\tau_1; x_1, t_1) \dots \mathcal{O}(\tau_n; x_n, t_n) \rangle^{\mathrm{con}}_{\mu}\}$ provides the cumulants of a probability distribution (see e.g. [1]). Hereafter the notation $\langle \dots \rangle_{\mu}$ denotes that both $\langle \dots \rangle_{\mu_+}$ and $\langle \dots \rangle_{\mu_-}$ are employed. When $\mathcal{O}$ is a current, this distribution fully describes the microscopic transport properties of the associated charge. For $n = 1$ and $n = 2$ one gets respectively the mean value and the quadratic fluctuations (quantum noise) of the current. In the following we consider operators whose one-point function $\langle \mathcal{O}(\tau; x, t) \rangle_{\mu}$ is independent of τ, as discussed in section 4.4.

JHEP08(2025)021

5.1 Charge and helicity transport

The mean values of the charge currents in (3.6) and (3.9) in the finite density representation of the CFT on the line can be written by using (4.1) and specialising the velocities to $V_+(u) = V_-(u)$ given by (4.7). The result is

$$\langle j_x(\tau;x,t)\rangle_\mu = \frac{\kappa}{2\pi}\left[\mu_+ V(u_+) - \mu_- V(u_-)\right] \tag{5.1}$$

$$\langle j_t(\tau;x,t)\rangle_\mu = \frac{\kappa}{2\pi}\left[\mu_+ V(u_+) + \mu_- V(u_-)\right]. \tag{5.2}$$

We remark that, instead, the mean values of the operators (3.12) and (3.13) vanish identically.

The mean values of the helicity currents (3.22) are obtained in the same way and read

$$\langle k_x(\tau;x,t)\rangle_\mu = \frac{\kappa}{2\pi}\left[\mu_+ V(u_+) + \mu_- V(u_-)\right] \tag{5.3}$$

$$\langle k_t(\tau;x,t)\rangle_\mu = \frac{\kappa}{2\pi}\left[\mu_+ V(u_+) - \mu_- V(u_-)\right]. \tag{5.4}$$

These mean values for the charge currents and for the helicity currents are independent of τ and the event with spacetime coordinates (x,t) corresponds to the initial point of the modular evolution; hence $(x,t) \in \mathcal{D}_A \cup \mathcal{R}_A$. We find it worth introducing the smooth planar vector fields $\boldsymbol{j}(x,t) \equiv \left(\langle j_x(\tau;x,t)\rangle_\mu, \langle j_t(\tau;x,t)\rangle_\mu\right)$ and $\boldsymbol{k}(x,t) \equiv \left(\langle k_x(\tau;x,t)\rangle_\mu, \langle k_t(\tau;x,t)\rangle_\mu\right)$ for $(x,t) \in \mathcal{D}_A \cup \mathcal{R}_A$. Despite the fact that these vector fields are defined in $\mathcal{D}_A \cup \mathcal{R}_A$, it is natural to extend them to the entire Minkowski spacetime and in the following such extension will be mainly explored. In figure 3 and figure 4 the vector fields $\boldsymbol{j}(x,t)$ and $\boldsymbol{k}(x,t)$ are displayed for a specific choice of the parameters (see the caption of figure 3). In particular, in the left panels $\mu_+ = \mu_-$, while $\mu_+ \neq \mu_-$ in the right panels. In figure 3, the top panels show $\boldsymbol{j}(x,t)$ for $(x,t) \in \mathcal{D}_A \cup \mathcal{R}_A$, while in the bottom panels the corresponding extensions to the entire Minkowski spacetime are displayed.

Two-dimensional vector fields have been largely explored [42, 43]. For instance, it is insightful to consider the critical points (also called singular points in the mathematical literature) of the vector field, i.e. the points where it vanishes. By construction, the critical points of both the vector fields $\boldsymbol{j}(x,t)$ and $\boldsymbol{k}(x,t)$ extended to the entire Minkowski spacetime are isolated points located in the vertices of the diamond $\mathcal{D}_A$, i.e. P_a, P_b, $P_{+\infty}$ and $P_{-\infty}$, whose light-cone coordinates are $(u_+,u_-) \in \{(a,a),(b,b),(b,a),(a,b)\}$ respectively (see the coloured dots in figure 3 and figure 4), which are obtained by combining the zeros of the function $V(u)$ in (4.7). Since a and b are zeros of (4.7) of order 1, all these critical points have multiplicity 1.

The Poincaré index is a useful tool to study smooth vector fields $\boldsymbol{v} \equiv (v_x, v_t)$ with isolated zeros. Given a smooth closed curve γ where the vector field is not vanishing, the Poincaré index of γ relative to the vector field $\boldsymbol{v}$ can be computed as follows

$$\mathcal{I}[\boldsymbol{v}](\gamma) \equiv \frac{1}{2\pi}\oint_\gamma \frac{v_t\,\mathrm{d}v_x - v_x\,\mathrm{d}v_t}{v_x^2 + v_t^2} \tag{5.5}$$

and it corresponds to the number of rotations in the positive (counterclockwise) direction that the vector field performs when we go around γ once. The index $\mathcal{I}_P$ of a critical point P

JHEP08(2025)021

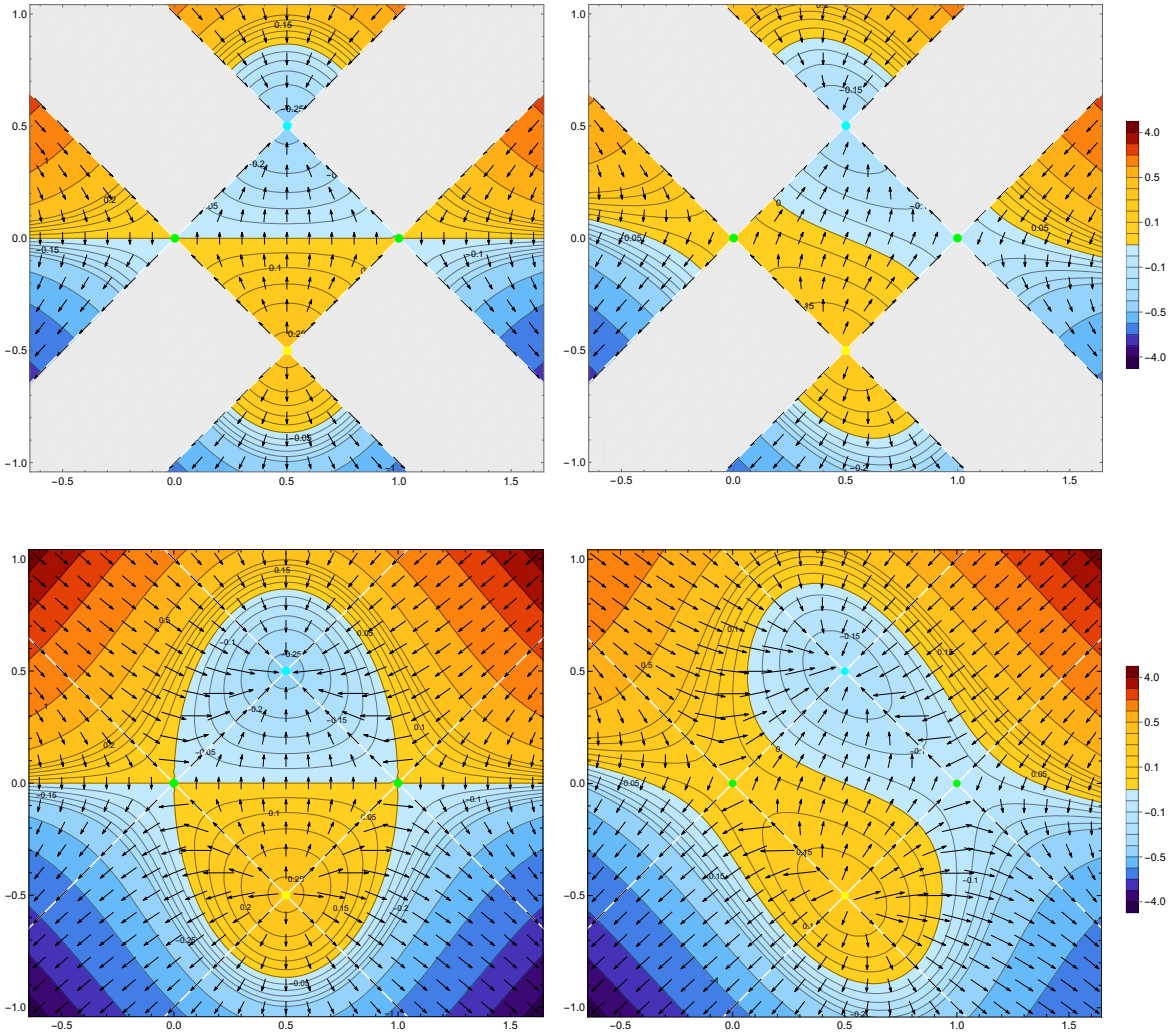

Figure 3. Vector fields for the mean values of the charge currents (5.1) and (5.2), whose potential is the first expressions in (5.12). The interval is $A = [0, 1]$ on the line and the CFT has $c = 1$, $\kappa = 3$ and either equal chemical potentials $\mu_+ = \mu_- = 0.52$ (left panels) or different chemical potentials $\mu_+ = 0.52$ and $\mu_- = 0.22$ (right panels). In the top panels the initial point $(x, t) \in \mathcal{D}_A \cup \mathcal{R}_A$, while in the bottom panels the vector field $\boldsymbol{j}(x, t)$ is extended to the entire Minkowski spacetime.

is the Poincaré index of a closed smooth curve that encloses only P; hence it is determined by the behaviour of the vector field nearby P. Depending on such behaviour, P is a critical point of certain type (e.g. either a node or a center or a focus or a saddle or something else). A node contains all the nearby trajectories and it is either stable or unstable, depending on whether all the trajectories move away from the point. A saddle has two transversal trajectories called separatices, one of which is ingoing and the other outgoing, while the other trajectories behave like a family of hyperbolas whose asymptotes are the separatrices. A node has Poincaré index $+1$ (like a focus and a center), while a saddle has Poincaré index -1. The vector fields $\boldsymbol{j}(x, t)$ and $\boldsymbol{k}(x, t)$ display two nodes, one stable and one unstable, and two saddles (in the bottom panels of figure 3 and figure 4, see the cyan dot, the yellow dot and the green dots respectively).

JHEP08(2025)021

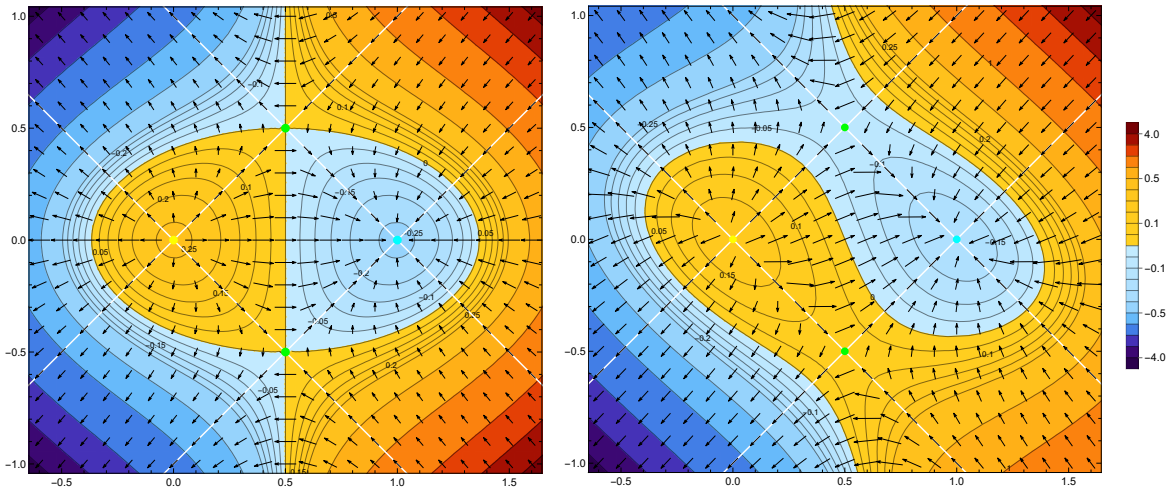

Figure 4. Vector fields for the mean values of the helicity currents (5.3) and (5.4), whose potential is the second expressions in (5.12), for either equal (left panel) or different (right panel) chemical potentials, in the same setup of figure 3.

Various theorems about the sum of the indices for smooth vector fields with isolated zeros have been established [42]. For instance, the index of a closed curve is equal to the sum of the indices of the critical points enclosed by the curve. A fundamental result in this context is the Poincaré-Hopf theorem, which claims that the sum of the indices of all the isolated critical points of a vector field on a two-dimensional compact manifold is independent of the vector field and equal to the Euler characteristic of the manifold. For the vector fields $\boldsymbol{j}(x,t)$ and $\boldsymbol{k}(x,t)$, which are defined on the plane, the sum of the indices of all the critical points is zero. These vector fields can be mapped to the Riemann sphere through the stereographic projection and the resulting vector fields on this compact manifold must have a critical point with Poincaré index +2 at the north pole, which corresponds to infinity on the plane.

By employing the definitions in (3.52), from (5.1)–(5.2) and (5.3)–(5.4) we introduce the local conductivities respectively as

$$\boldsymbol{\sigma}_{j,e} \equiv \partial_{\mu_e} \boldsymbol{j}(x,t) = \frac{\kappa}{4\pi} \Big(V(u_+) - V(u_-)\,,\, V(u_+) + V(u_-) \Big) \tag{5.6}$$

$$\boldsymbol{\sigma}_{j,h} \equiv \partial_{\mu_h} \boldsymbol{j}(x,t) = \frac{\kappa}{4\pi} \Big(V(u_+) + V(u_-)\,,\, V(u_+) - V(u_-) \Big) \tag{5.7}$$

and

$$\boldsymbol{\sigma}_{k,e} \equiv \partial_{\mu_e} \boldsymbol{k}(x,t) = \boldsymbol{\sigma}_{j,h} \qquad\qquad \boldsymbol{\sigma}_{k,h} \equiv \partial_{\mu_h} \boldsymbol{k}(x,t) = \boldsymbol{\sigma}_{j,e}\,. \tag{5.8}$$

These four local conductivities are independent of τ; hence their Fourier transform gives only a Dirac delta term.

In order to understand the nature of the modular transport, let us consider

$$\int_0^\tau \boldsymbol{j}(x,t)\,\mathrm{d}\tilde{\tau} = \boldsymbol{j}(x,t)\,\tau \qquad\qquad \int_0^\tau \boldsymbol{k}(x,t)\,\mathrm{d}\tilde{\tau} = \boldsymbol{k}(x,t)\,\tau\,. \tag{5.9}$$

These linear growths tell us that the modular transport is ballistic (see e.g. [44]). We remark that the linear response approximation is not employed here.

JHEP08(2025)021

A vector field $\boldsymbol{v}$ has vanishing curl when its components satisfy $\partial_t v_x - \partial_x v_t = 0$ and this feature implies that it can be written as the gradient of the potential W, namely $v_\mu = -\partial_\mu \mathsf{W}$.

Both the vector fields $\boldsymbol{j}(x,t)$ and $\boldsymbol{k}(x,t)$ have vanishing curl and therefore the corresponding potentials $\mathsf{W}_j(x,t)$ and $\mathsf{W}_k(x,t)$ respectively can be obtained. Indeed, we find that

$$\langle j_x(\tau;x,t)\rangle_\mu = -\partial_x \mathsf{W}_j(x,t) \qquad \langle j_t(\tau;x,t)\rangle_\mu = -\partial_t \mathsf{W}_j(x,t) \tag{5.10}$$

and

$$\langle k_x(\tau;x,t)\rangle_\mu = -\partial_x \mathsf{W}_k(x,t) \qquad \langle k_t(\tau;x,t)\rangle_\mu = -\partial_t \mathsf{W}_k(x,t) \tag{5.11}$$

where the potentials W_j and W_k are defined respectively as

$$\mathsf{W}_j(x,t) \equiv \frac{\kappa}{2\pi}\left[\mu_+ g(u_+) - \mu_- g(u_-)\right] \qquad \mathsf{W}_k(x,t) \equiv \frac{\kappa}{2\pi}\left[\mu_+ g(u_+) + \mu_- g(u_-)\right] \tag{5.12}$$

in terms of

$$g(u) \equiv \frac{2\pi}{3(b-a)}\left(u - \frac{a+b}{2}\right)\left(u^2 - (a+b)\,u - \frac{a^2 - 4ab + b^2}{2}\right). \tag{5.13}$$

The arbitrary additive constants in (5.12) have been fixed by imposing the vanishing condition at the center of $\mathcal{D}_A$ for both these potentials; indeed (5.13) has a zero at $u = (a+b)/2$. We remark that (5.1)–(5.2), (5.3)–(5.4) are consistent with (5.10) and (5.11) because

$$-\partial_u g(u) = V(u)\,. \tag{5.14}$$

Given a curve γ (not necessarily closed) parameterised by s, let us denote the line integral of the vector field $\boldsymbol{v}$ along γ and the flux of $\boldsymbol{v}$ through γ respectively as

$$\mathcal{L}[\boldsymbol{v}](\gamma) \equiv \int_\gamma \boldsymbol{v}\cdot\hat{\boldsymbol{\tau}}\,\mathrm{d}s \qquad \mathcal{F}[\boldsymbol{v}](\gamma) \equiv \int_\gamma \boldsymbol{v}\cdot\hat{\boldsymbol{n}}\,\mathrm{d}s \tag{5.15}$$

where $\hat{\boldsymbol{\tau}}$ and $\hat{\boldsymbol{n}}$ are the unit vectors which are respectively tangent and normal to γ.

We highlight the vanishing of the fluxes of the vector fields $\boldsymbol{j}(x,t)$ and $\boldsymbol{k}(x,t)$ through the straight white lines in figure 3 and figure 4, which identify the diamond $\mathcal{D}_A$ and the region $\mathcal{R}_A$ (i.e. the grey and light blue regions in figure 1). This can be shown by observing that the absolute value of the ratio of theirs components is equal to one along these lines. This absence of flux naturally suggests to consider the total charges in the diamond $\mathcal{D}_A$. In the finite density representation, by using (4.1) and (3.52), for the mean values of (3.17) and (3.23) we find respectively

$$\langle Q_A\rangle_\mu = -\frac{\kappa}{4\pi}\,\mu_e\,\ell^2 \qquad \langle \widetilde{Q}_A\rangle_\mu = -\frac{\kappa}{4\pi}\,\mu_h\,\ell^2\,. \tag{5.16}$$

A crucial feature of $\boldsymbol{j}(x,t)$ and $\boldsymbol{k}(x,t)$ is that they are curl free vector fields. The Green theorem implies that any line integral of a curl free vector field along a closed curve vanishes; hence, all the line integrals along curves anchored to the same endpoints provide the same result given by the difference between the values of the potential at these endpoints. In our case, we find it worth considering the lines anchored to the opposite vertices of $\mathcal{D}_A$ and, among them, the convenient representatives to choose are the horizontal segment

JHEP08(2025)021

$A = \{(x, t = 0)\,;\, a \leqslant x \leqslant b\}$ along the real axis, whose endpoints are P_a and P_b, and the vertical segment $\tilde{A} = \{(x = \frac{a+b}{2}, t)\,;\, -\frac{b-a}{2} \leqslant t \leqslant \frac{b-a}{2}\}$ on the imaginary axis, whose endpoints are $P_{-\infty}$ and $P_{+\infty}$. Given a smooth curves $\gamma(P_1 \to P_2)$ starting in P_1 and ending in P_2 and a vector field $\boldsymbol{v}(x,t)$, let us denote by $\mathcal{L}[\boldsymbol{v}](\gamma(P_1 \to P_2))$ the line integral of $\boldsymbol{v}(x,t)$ along $\gamma(P_1 \to P_2)$ and by $\mathcal{F}[\boldsymbol{v}](\gamma(P_1 \to P_2))$ its flux through $\gamma(P_1 \to P_2)$. When $\boldsymbol{v}(x,t)$ is curl free, $\mathcal{L}[\boldsymbol{v}](\gamma(P_1 \to P_2))$ depends only on the endpoints P_1 and P_2. For the vector field $\boldsymbol{j}(x,t)$ in (5.1)–(5.2), these line integrals can be written in terms of the mean values of total charges (5.16) as follows

$$\mathcal{L}[\boldsymbol{j}](\gamma(P_a \to P_b)) = \mathsf{W}_j\big|_{P_a} - \mathsf{W}_j\big|_{P_b} = -\frac{2\pi}{3}\,\langle \widetilde{Q}_A \rangle_\mu \tag{5.17}$$

$$\mathcal{L}[\boldsymbol{j}](\gamma(P_{-\infty} \to P_{+\infty})) = \mathsf{W}_j\big|_{P_{-\infty}} - \mathsf{W}_j\big|_{P_{+\infty}} = -\frac{2\pi}{3}\,\langle Q_A \rangle_\mu \tag{5.18}$$

and, similarly, for the vector field $\boldsymbol{k}(x,t)$ in (5.3)–(5.4) we have that

$$\mathcal{L}[\boldsymbol{k}](\gamma(P_a \to P_b)) = \mathsf{W}_k\big|_{P_a} - \mathsf{W}_k\big|_{P_b} = -\frac{2\pi}{3}\,\langle Q_A \rangle_\mu \tag{5.19}$$

$$\mathcal{L}[\boldsymbol{k}](\gamma(P_{-\infty} \to P_{+\infty})) = \mathsf{W}_k\big|_{P_{-\infty}} - \mathsf{W}_k\big|_{P_{+\infty}} = -\frac{2\pi}{3}\,\langle \widetilde{Q}_A \rangle_\mu\,. \tag{5.20}$$

When $\mu_+ = \mu_-$, the line integrals in (5.17) and (5.20) vanish, as one can observe also from the left panel of figure 3 and figure 4 respectively.

We find it worth studying also the fluxes of the vector fields $\boldsymbol{j}(x,t)$ and $\boldsymbol{k}(x,t)$ through the above mentioned curves. However, since the divergence of these vector fields does not vanish, these fluxes depend on the curve. Among the curves starting in P_a and ending in P_b, let us consider the spacelike curve γ_{t_0} given by (4.15) with $u_\pm = \frac{a+b}{2} \pm t_0$ and $-\ell/2 \leqslant t_0 \leqslant \ell/2$. Analogously, in the class of curves starting in $P_{-\infty}$ and ending in $P_{+\infty}$, we choose the modular trajectories γ_{x_0} given by (4.13) with $u_\pm = x_0$ and $a \leqslant x_0 \leqslant b$. The fluxes of $\boldsymbol{j}(x,t)$ through these curves can be written in terms of the mean values of total charges (5.16) as follows

$$\mathcal{F}[\boldsymbol{j}](\gamma_{t_0}(P_a \to P_b)) = \frac{2\pi}{3}\,\langle Q_A \rangle_\mu\, f(2t_0/\ell) \tag{5.21}$$

$$\mathcal{F}[\boldsymbol{j}](\gamma_{x_0}(P_{-\infty} \to P_{+\infty})) = \frac{2\pi}{3}\,\langle \widetilde{Q}_A \rangle_\mu\, f\big(2(x_0 - \tfrac{a+b}{2})/\ell\big) \tag{5.22}$$

and, similarly, for the fluxes of $\boldsymbol{k}(x,t)$ we get

$$\mathcal{F}[\boldsymbol{k}](\gamma_{t_0}(P_a \to P_b)) = \frac{2\pi}{3}\,\langle \widetilde{Q}_A \rangle_\mu\, f(2t_0/\ell) \tag{5.23}$$

$$\mathcal{F}[\boldsymbol{k}](\gamma_{x_0}(P_{-\infty} \to P_{+\infty})) = \frac{2\pi}{3}\,\langle Q_A \rangle_\mu\, f\big(2(x_0 - \tfrac{a+b}{2})/\ell\big) \tag{5.24}$$

where the function $f(y)$ is defined for $|y| < 1$ as

$$f(y) \equiv \frac{3(1-y^2)^2}{8\,y^3}\left[\left(1+y^2\right)\log\left(\frac{1+y}{1-y}\right) - 2y\right]. \tag{5.25}$$

Notice that this function is even, vanishes as $|y| \to 1$ and takes its maximum value equal to 1 at $y = 0$.

JHEP08(2025)021

Focussing on the case $\mu_+ = \mu_-$ considered in the left panel figure 3 for simplicity, which has already non trivial modular transport properties, a heuristic physical picture for the charge transport in the diamond $\mathcal{D}_A$ is the following. The critical points $P_{-\infty}$ and $P_{+\infty}$ play the role of a source and a sink respectively: the charged excitations are emitted by $P_{-\infty}$ and absorbed by $P_{+\infty}$ with vanishing velocity. Since the total charge in $\mathcal{D}_A$ is conserved (see (5.16)), the amount of charge emitted in $P_{-\infty}$ is equal to the one absorbed in $P_{+\infty}$. After the emission, in the lower part of $\mathcal{D}_A$, where $t < 0$, the charges are accelerated, arriving at the segment A on the x-axes with maximal velocity. The flux through A, which is given by (5.21) for $t_0 = 0$, is maximal. In the upper part of $\mathcal{D}_A$, where $t > 0$, the charges decelerate until they reach $P_{+\infty}$, where they are absorbed. When $\mu_+ \neq \mu_-$ the situation is similar, but deformed as shown in the right panel of figure 3 for a specific setup. In this case the maximum flux should be reached along the curve separating the light blue and the orange regions, where the potential vanishes.

A similar heuristic picture for the helicity transport (see figure 4) is obtained by adapting the above observations properly. For instance, in this case the vertices P_a and P_b of the diamond $\mathcal{D}_A$ play the role of the source and the sink respectively and, when $\mu_+ = \mu_-$, the maximal flux corresponds to $\tilde{A}$.

We find it worth mentioning that the charge transport displayed in the left panel of figure 3 resembles the transport of electrons in the vacuum tube called triode in the context of electromagnetism. In this analogy, $P_{-\infty}$ and $P_{+\infty}$ play the role of the cathode and anode respectively. Indeed, the cathode emits electrons, which are accelerated by the electric field in the vacuum. The control grid of the triode is represented by the segment A at $t = 0$ and its potential is tuned in such a way that the electrons produced by the cathode in $P_{-\infty}$ reach the anode in $P_{+\infty}$ with vanishing velocity.

5.2 Energy and momentum transport

The analysis discussed in section 5.1 can be adapted to the energy and momentum currents.

The mean values of the energy currents (3.29)–(3.30) specialised to $V_+(u) = V_-(u)$ given by (4.7) are obtained by employing (4.1) and the results read respectively

$$\langle \mathcal{J}_x(\tau; x, t) \rangle_\mu = -\frac{\kappa}{4\pi} \left[\mu_+^2 V(u_+)^2 - \mu_-^2 V(u_-)^2 \right] \tag{5.26}$$

$$\langle \mathcal{J}_t(\tau; x, t) \rangle_\mu = -\frac{\kappa}{4\pi} \left[\mu_+^2 V(u_+)^2 + \mu_-^2 V(u_-)^2 \right] \tag{5.27}$$

where we fixed the constant $C_{\mathcal{J}} = -\pi c/6$ to get the last expression. This constant has been determined by observing that for (4.7) we have

$$V(u)^2 \, \mathcal{V}[V](u) = -2\pi^2 \tag{5.28}$$

which implies that the term in the second line of (3.30) drastically simplifies to

$$-\frac{c}{24\pi} \left\{ V(u_+)^2 \, \mathcal{V}[V](u_+) + V(u_-)^2 \, \mathcal{V}[V](u_-) \right\} = \frac{\pi \, c}{6} \tag{5.29}$$

and imposing the vanishing of the final expression at all the vertices of $\mathcal{D}_A$. The mean values (5.26) and (5.27) provide the components of the planar vector field $\boldsymbol{\mathcal{J}}(x, t)$.

JHEP08(2025)021

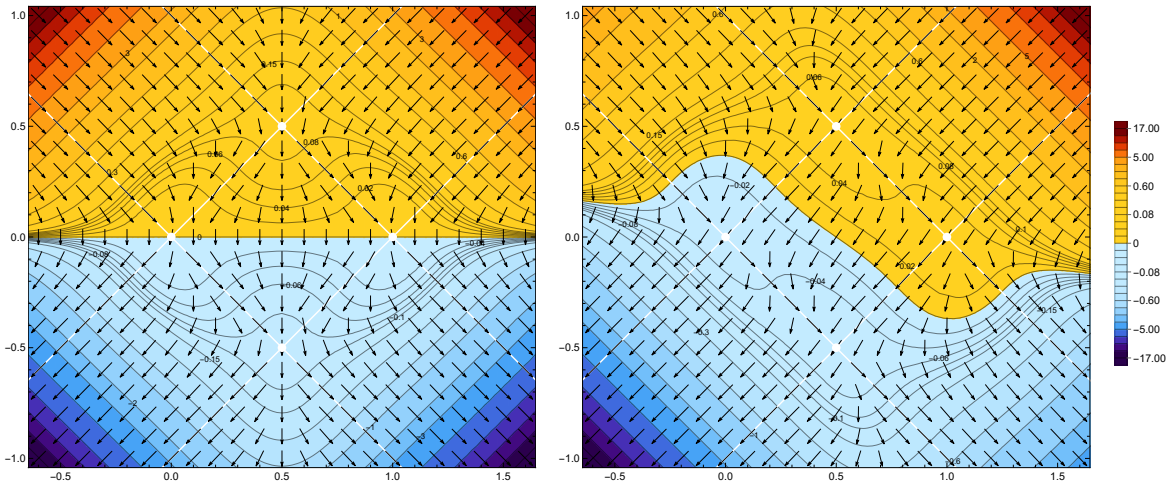

Figure 5. Vector fields for the mean values of the energy density currents (5.26) and (5.27), whose potential is the first expressions in (5.38), for either equal (left panel) or different (right panel) chemical potentials, in the same setup of figure 3.

Similarly, we introduce the planar vector field $\widetilde{\mathcal{J}}(x,t)$ whose components are the mean values of the momentum currents (3.37) and (3.38), which are obtained through the same steps[3] and read respectively

$$\langle \widetilde{\mathcal{J}}_x(\tau;x,t)\rangle_\mu = -\frac{\kappa}{4\pi}\left[\,\mu_+^2 V(u_+)^2 + \mu_-^2 V(u_-)^2\,\right] \tag{5.30}$$

$$\langle \widetilde{\mathcal{J}}_t(\tau;x,t)\rangle_\mu = -\frac{\kappa}{4\pi}\left[\,\mu_+^2 V(u_+)^2 - \mu_-^2 V(u_-)^2\,\right]. \tag{5.31}$$

The planar vector fields $\mathcal{J}(x,t)$ and $\widetilde{\mathcal{J}}(x,t)$ are displayed in figure 5 and figure 6 for the choice parameters reported in the caption of figure 3. In particular, $\mu_+ = \mu_-$ in the left panels, while $\mu_+ \neq \mu_-$ in the right panels. These vector fields have the same isolated critical points which are given by the vertices of the diamond $\mathcal{D}_A$. All of them have multiplicity 2 and Poincaré index 0. By applying the Poincaré-Hopf theorem (see section 5.1), we find consistency with the fact that these vector fields can me mapped (through the stereographic projection) to vector fields on the Riemann sphere which have a critical point of index 2 at the north pole.

The fluxes of the vector fields $\mathcal{J}(x,t)$ and $\widetilde{\mathcal{J}}(x,t)$ through the straight white lines in figure 5 and figure 6 vanish. Indeed, the absolute value of the ratios of their components is equal to 1 along these lines. Unfortunately, this analytic result is not properly shown in figure 5 and figure 6 because of a graphical failure in the displaying of these vector fields around their critical points. Another similar failure occurs at the vertices of $\mathcal{D}_A$, where arrows are displayed, while they should not because they are critical points of the vector fields. These failures could be related to the multiplicity of the critical points; indeed they do not occur for the vector fields shown in figure 3 and figure 4, whose critical points have multiplicity 1.

[3] In this case $C_{\widetilde{\mathcal{J}}} = 0$ since, from (5.28) we have that $V(u_+)^2\,\mathcal{V}[V](u_+) - V(u_-)^2\,\mathcal{V}[V](u_-) = 0$, which occurs because the central charge is the same for the two chiralities (see (2.1)).

JHEP08(2025)021

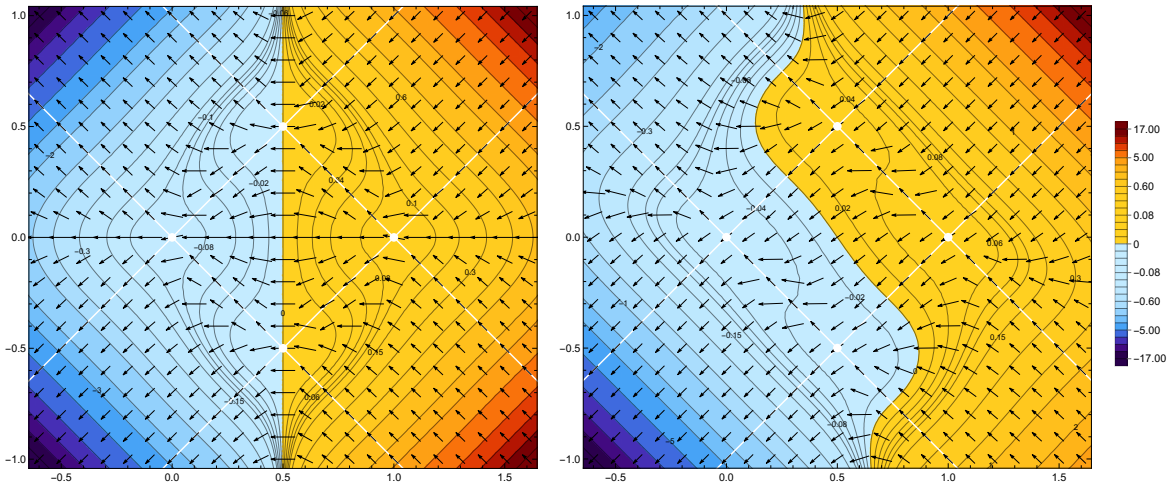

Figure 6. Vector fields for the mean values of the momentum density currents (5.30) and (5.31), whose potential is the second expressions in (5.38), for either equal (left panel) or different (right panel) chemical potentials, in the same setup of figure 3.

The local conductivities corresponding to (5.26)–(5.27) and (5.30)–(5.31) are respectively

$$\boldsymbol{\sigma}_{\mathcal{J},e} \equiv \partial_{\mu_e}\boldsymbol{\mathcal{J}}(x,t) = -\frac{\kappa}{4\pi}\left(\mu_+ V(u_+)^2 - \mu_- V(u_-)^2\,,\,\mu_+ V(u_+)^2 + \mu_- V(u_-)^2\right) \tag{5.32}$$

$$\boldsymbol{\sigma}_{\mathcal{J},h} \equiv \partial_{\mu_h}\boldsymbol{\mathcal{J}}(x,t) = -\frac{\kappa}{4\pi}\left(\mu_+ V(u_+)^2 + \mu_- V(u_-)^2\,,\,\mu_+ V(u_+)^2 - \mu_- V(u_-)^2\right) \tag{5.33}$$

and

$$\boldsymbol{\sigma}_{\widetilde{\mathcal{J}},e} \equiv \partial_{\mu_e}\widetilde{\boldsymbol{\mathcal{J}}}(x,t) = \boldsymbol{\sigma}_{\mathcal{J},h} \qquad \boldsymbol{\sigma}_{\widetilde{\mathcal{J}},h} \equiv \partial_{\mu_h}\widetilde{\boldsymbol{\mathcal{J}}}(x,t) = \boldsymbol{\sigma}_{\mathcal{J},e} \tag{5.34}$$

which are independent of τ; hence their Fourier transform gives only a Dirac delta term.

The ballistic nature of the modular transport observed through (5.9) is confirmed by the linear growth in τ of the following quantities

$$\int_0^\tau \boldsymbol{\mathcal{J}}(x,t)\,\mathrm{d}\tilde{\tau} = \boldsymbol{\mathcal{J}}(x,t)\,\tau \qquad \int_0^\tau \widetilde{\boldsymbol{\mathcal{J}}}(x,t)\,\mathrm{d}\tilde{\tau} = \widetilde{\boldsymbol{\mathcal{J}}}(x,t)\,\tau\,. \tag{5.35}$$

Both the vector fields defined by the energy and momentum currents are curl free and can be written as the gradient some potentials as follows

$$\langle \mathcal{J}_x(\tau;x,t)\rangle_\mu = -\,\partial_x \mathsf{W}_{\mathcal{J}}(x,t) \qquad \langle \mathcal{J}_t(\tau;x,t)\rangle_\mu = -\,\partial_t \mathsf{W}_{\mathcal{J}}(x,t) \tag{5.36}$$

and

$$\langle \widetilde{\mathcal{J}}_x(\tau;x,t)\rangle_\mu = -\,\partial_x \mathsf{W}_{\widetilde{\mathcal{J}}}(x,t) \qquad \langle \widetilde{\mathcal{J}}_t(\tau;x,t)\rangle_\mu = -\,\partial_t \mathsf{W}_{\widetilde{\mathcal{J}}}(x,t) \tag{5.37}$$

For the potentials $\mathsf{W}_{\mathcal{J}}$ and $\mathsf{W}_{\widetilde{\mathcal{J}}}$, we find respectively

$$\mathsf{W}_{\mathcal{J}}(x,t) \equiv \frac{\kappa}{4\pi}\left[\mu_+^2 G(u_+) - \mu_-^2 G(u_-)\right] \qquad \mathsf{W}_{\widetilde{\mathcal{J}}}(x,t) \equiv \frac{\kappa}{4\pi}\left[\mu_+^2 G(u_+) + \mu_-^2 G(u_-)\right] \tag{5.38}$$

being $G(u)$ defined as

$$\begin{aligned} G(u) \equiv \frac{2\pi^2}{15\,(b-a)^2}\left(u - \frac{a+b}{2}\right)\Big[\,&6\,u^4 - 12(a+b)\,u^3 + 4(a^2+7ab+b^2)\,u^2 \\ &+ 2(a^3 - 7a^2b - 7ab^2 + b^3)\,u + a^4 - 6a^3b + 16a^2b^2 - 6ab^3 + b^4\Big] \end{aligned} \tag{5.39}$$

JHEP08(2025)021

whose additive constant has been fixed by imposing the condition $G(\frac{a+b}{2}) = 0$. The expressions (5.26)–(5.27), (5.30)–(5.31), (5.36) and (5.37) are consistent because (5.39) and (4.7) are related as follows

$$\partial_u G(u) = V(u)^2 \,. \tag{5.40}$$

Finally, since the vector fields $\boldsymbol{\mathcal{J}}(x,t)$ and $\widetilde{\boldsymbol{\mathcal{J}}}(x,t)$ are curl free, their line integrals along a curve depend only on the endpoints of the curve. Let us consider the curves anchored to the opposite vertices of $\mathcal{D}_A$, as done in section 5.1. By employing (5.36) and (5.37), we find

$$\mathcal{L}[\boldsymbol{\mathcal{J}}](\gamma(P_a \to P_b)) = \mathsf{W}_{\mathcal{J}}|_{P_a} - \mathsf{W}_{\mathcal{J}}|_{P_b} = -\frac{4\pi}{5}\,\widetilde{\mathsf{E}}_A \tag{5.41}$$

$$\mathcal{L}[\boldsymbol{\mathcal{J}}](\gamma(P_{-\infty} \to P_{+\infty})) = \mathsf{W}_{\mathcal{J}}|_{P_{-\infty}} - \mathsf{W}_{\mathcal{J}}|_{P_{+\infty}} = -\frac{4\pi}{5}\,\mathsf{E}_A \tag{5.42}$$

and

$$\mathcal{L}[\widetilde{\boldsymbol{\mathcal{J}}}](\gamma(P_a \to P_b)) = \mathsf{W}_{\widetilde{\mathcal{J}}}|_{P_a} - \mathsf{W}_{\widetilde{\mathcal{J}}}|_{P_b} = -\frac{4\pi}{5}\,\mathsf{E}_A \tag{5.43}$$

$$\mathcal{L}[\widetilde{\boldsymbol{\mathcal{J}}}](\gamma(P_{-\infty} \to P_{+\infty})) = \mathsf{W}_{\widetilde{\mathcal{J}}}|_{P_{-\infty}} - \mathsf{W}_{\widetilde{\mathcal{J}}}|_{P_{+\infty}} = -\frac{4\pi}{5}\,\widetilde{\mathsf{E}}_A \tag{5.44}$$

where we have introduced

$$\mathsf{E}_A \equiv \frac{\kappa}{24}(\mu_+^2 + \mu_-^2)\,\ell^3 \qquad\qquad \widetilde{\mathsf{E}}_A \equiv \frac{\kappa}{24}(\mu_+^2 - \mu_-^2)\,\ell^3 \tag{5.45}$$

which correspond respectively to the mean value of the total energy (3.32) and of the total momentum (3.39) in the diamond $\mathcal{D}_A$ in the case where $f_+(u_+) = f_-(u_-) = 0$ are imposed. Instead, from (4.6) we have that the mean values of (3.32) and (3.39) are $\langle E_A \rangle_\mu = \langle \widetilde{E}_A \rangle_\mu = 0$.

The vanishing of the line integrals in (5.42) and (5.44) for $\mu_+ = \mu_-$ can be observed also from the left panel of figure 5 and figure 6 respectively.

We find it worth considering also the fluxes of $\boldsymbol{\mathcal{J}}(x,t)$ and $\widetilde{\boldsymbol{\mathcal{J}}}(x,t)$ through the curves γ_{t_0} and γ_{x_0} introduced in section 5.1. They can be written as

$$\mathcal{F}[\boldsymbol{\mathcal{J}}](\gamma_{t_0}(P_a \to P_b)) = -\frac{4\pi}{5}\,\mathsf{E}_A\, F(2t_0/\ell) \tag{5.46}$$

$$\mathcal{F}[\boldsymbol{\mathcal{J}}](\gamma_{x_0}(P_{-\infty} \to P_{+\infty})) = -\frac{4\pi}{5}\,\widetilde{\mathsf{E}}_A\, F(2(x_0 - \tfrac{a+b}{2})/\ell) \tag{5.47}$$

and

$$\mathcal{F}[\widetilde{\boldsymbol{\mathcal{J}}}](\gamma_{t_0}(P_a \to P_b)) = -\frac{4\pi}{5}\,\widetilde{\mathsf{E}}_A\, F(2t_0/\ell) \tag{5.48}$$

$$\mathcal{F}[\widetilde{\boldsymbol{\mathcal{J}}}](\gamma_{x_0}(P_{-\infty} \to P_{+\infty})) = -\frac{4\pi}{5}\,\mathsf{E}_A\, F(2(x_0 - \tfrac{a+b}{2})/\ell) \tag{5.49}$$

in terms of the mean values of total charges (5.45), where $F(y)$ is defined for $|y| < 1$ as follows

$$F(y) \equiv \frac{5\,(1-y^2)^2}{64\,y^5}\left[2y(3y^4 - 2y^2 + 3) - 3\left(1-y^2\right)^2\left(1+y^2\right)\log\left(\frac{1+y}{1-y}\right)\right]. \tag{5.50}$$

This function is even, vanishes as $|y| \to 1$ and takes its maximum value equal to 1 at $y = 0$.

JHEP08(2025)021

5.3 Quantum noise

Quantum effects along the conventional temporal evolution of any observable $\mathcal{O}$ generate non-trivial fluctuations around its mean value $\langle\mathcal{O}\rangle$. This is the case for the modular evolution as well. For instance, the quadratic fluctuations of the current $j_x(\tau;x,t)$ describe the quantum noise produced by the transport of charged particles. It is known [45, 46] that, besides spoiling the charge propagation and detection, the noise carries also useful information because it provides the experimental basis of noise spectroscopy.

The basic quantity of interest is the (modular) noise power generated by the charge current (3.6) at frequency ω in the point (x,t) of the spacetime, defined as follows

$$P_j(\omega;x,t) \equiv -\int_{-\infty}^{\infty} \langle j_x(\tau_1;x,t)\, j_x(\tau_2;x,t)\rangle_\mu^{\text{con}}\, \mathrm{e}^{\mathrm{i}\omega\tau_{12}}\, \mathrm{d}\tau_{12}\,. \tag{5.51}$$

Since τ_{12} is dimensionless, the corresponding frequency ω is dimensionless as well. Notice that the noise power is generated only by j_x because $\langle j_t(\tau_1;x,t)\, j_t(\tau_2;x,t)\rangle_\mu^{\text{con}}$ vanishes identically. Indeed, j_t introduced in (3.9) is proportional to the identity operator, being generated only by the central extension κ in the r.h.s. of (2.5).

Considering (3.13), we remark that $\langle j_x(\tau_1;x,t)\, j_x(\tau_2;x,t)\rangle_\mu^{\text{con}} = \langle \hat{j}_x(\tau_1;x,t)\, \hat{j}_x(\tau_2;x,t)\rangle_\mu^{\text{con}}$; indeed $j_x(\tau;x,t)$ and $\hat{j}_x(\tau;x,t)$ differ by a real function.

By using (3.6), the modular noise power can be expressed in terms of the two-point functions of the chiral currents $j_\pm(\tau,u)$

$$\begin{aligned} P_j(\omega;x,t) = -\int_{-\infty}^{\infty} \Big[& V(u_+)^2\, \langle j_+(\tau_1,u_+)\, j_+(\tau_2,u_+)\rangle_{\mu_+}^{\text{con}} \\ & + V(u_-)^2\, \langle j_-(\tau_1,u_-)\, j_-(\tau_2,u_-)\rangle_{\mu_-}^{\text{con}} \Big] \mathrm{e}^{\mathrm{i}\omega\tau_{12}}\, \mathrm{d}\tau_{12}\,. \end{aligned} \tag{5.52}$$

By employing (4.47) and the limit given in (4.50), we have that the dependence on $V(u_+)$ and $V(u_-)$ drops out and therefore (5.52) becomes (see (F.3) for the evaluation of the integral)

$$\begin{aligned} P_j(\omega;x,t) &= -\frac{\kappa}{4} \lim_{\varepsilon\to 0} \int_{-\infty}^{\infty} \left[\frac{1}{\sinh^2(\pi\tau - \mathrm{i}\varepsilon)} + \frac{1}{\sinh^2(-\pi\tau + \mathrm{i}\varepsilon)} \right] \mathrm{e}^{\mathrm{i}\omega\tau}\, \mathrm{d}\tau \\ &= -\frac{\kappa}{2} \lim_{\varepsilon\to 0} \int_{-\infty}^{\infty} \frac{\mathrm{e}^{\mathrm{i}\omega\tau}}{\sinh^2(\pi\tau - \mathrm{i}\varepsilon)}\, \mathrm{d}\tau = \frac{\kappa}{2\pi}\, \omega \coth(\omega/2) + \frac{\kappa}{2\pi}\, \omega \end{aligned} \tag{5.53}$$

which is indepedent of x and t. The zero frequency limit of (5.53) reads

$$P_j(0;x,t) = \lim_{\omega\to 0} P_j(\omega;x,t) = \frac{\kappa}{\pi}\,. \tag{5.54}$$

It is worth comparing this result with the Johnson-Nyquist law [47, 48]. In a CFT on the line at finite inverse temperature β and vanishing chemical potential, the two-point functions of the chiral currents read

$$\langle j_\pm(u)\, j_\pm(v)\rangle_\beta^{\text{con}} = \frac{\kappa}{4\pi^2} \left(\frac{\pi}{\beta\, \sinh[\pi(u-v\mp\mathrm{i}\varepsilon)/\beta]} \right)^2. \tag{5.55}$$

Since $\varrho(x,t) = j_+(u_+) + j_-(u_-)$, $j_x(x,t) = j_+(u_+) - j_-(u_-)$ and $\langle j_\pm(u)\, j_\mp(v)\rangle_\beta^{\text{con}} = 0$, by using (F.3) the noise power $P_{\text{JN}}(\omega)$ at frequency ω in the point x of the space for ϱ and

JHEP08(2025)021